Particle Detection: Trackers

Lecture 3

Gregor Herten

University of Freiburg, Germany

11. June 2009

CERN-FNAL HCP School 2009

Outline

Lecture 1

1. Interaction of charged particle with matter
2. Momentum measurement
3. Drift and Diffusion in Gases
4. History of Tracking Detectors
5. Proportional Chambers

Lecture 2

6. Drift Chambers
7. Micro Pattern Gas Chambers
8. Limitations of Gaseous Detectors

Lecture 3

9. Vertex Reconstruction
10. Semiconductor Detectors
11. Silicon Strip and Pixel Detectors
12. Radiation Damage of Silicon Detectors
13. New Semiconductor Detector Concepts
14. Tracking Systems: ATLAS, CMS

9. Need for semiconductor tracker: Vertex Reconstruction

$$B_s^0 \to \psi'(\to \mu^+\mu^-)\phi(\to KK)$$

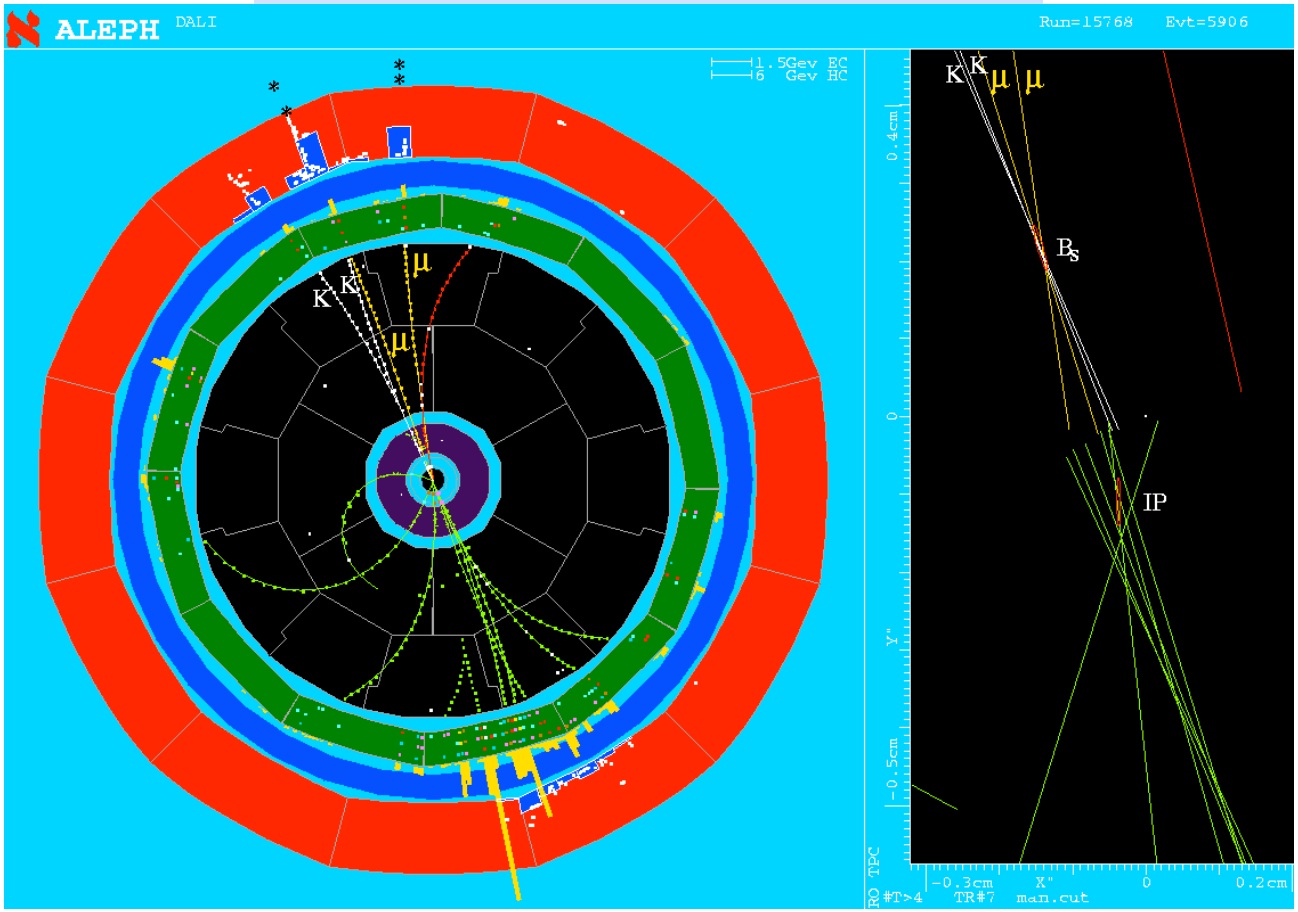

Aleph event:

Fully reconstructed B_s decay.

10 m

0.5 mm

Track measurements with a precision of a few μm near the interaction point improve the momentum measurement and allow to determine the decay vertex, especially important for bottom hadrons.

9. Vertex Reconstruction

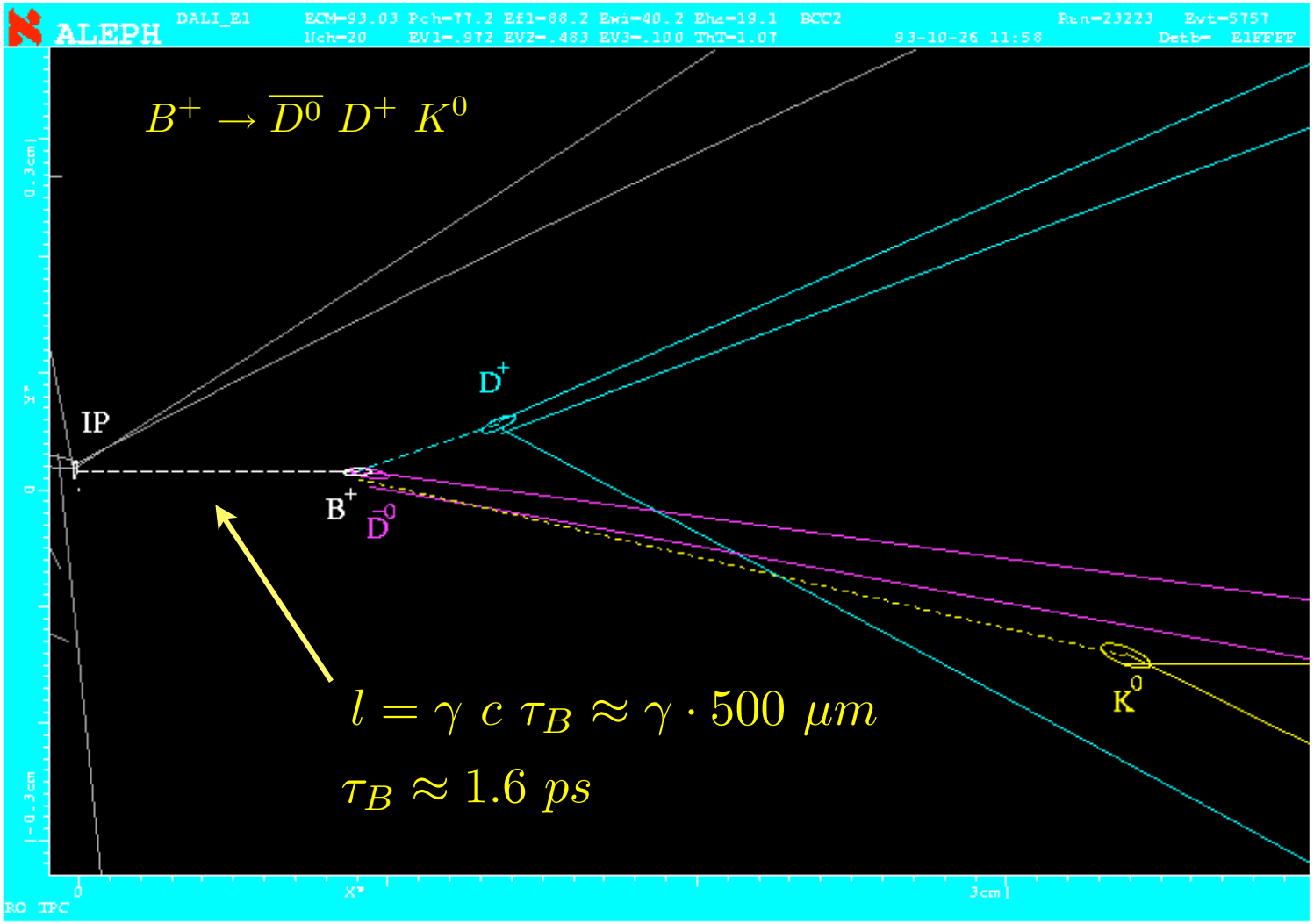

The life time of B-mesons can be measured from the decay length l, if the momentum of the B-meson (γ-factor) is measured as well.

Impact parameter resolution (simplified)

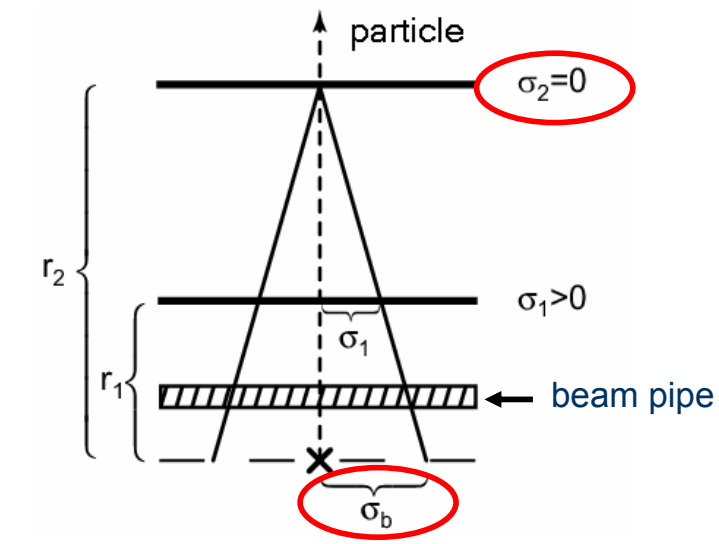

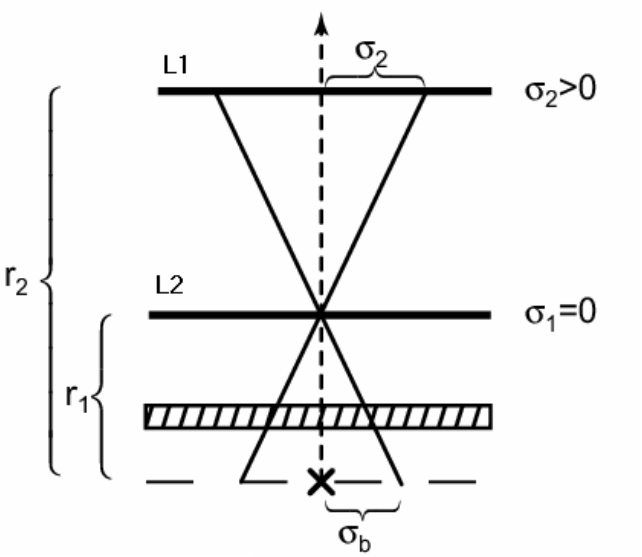

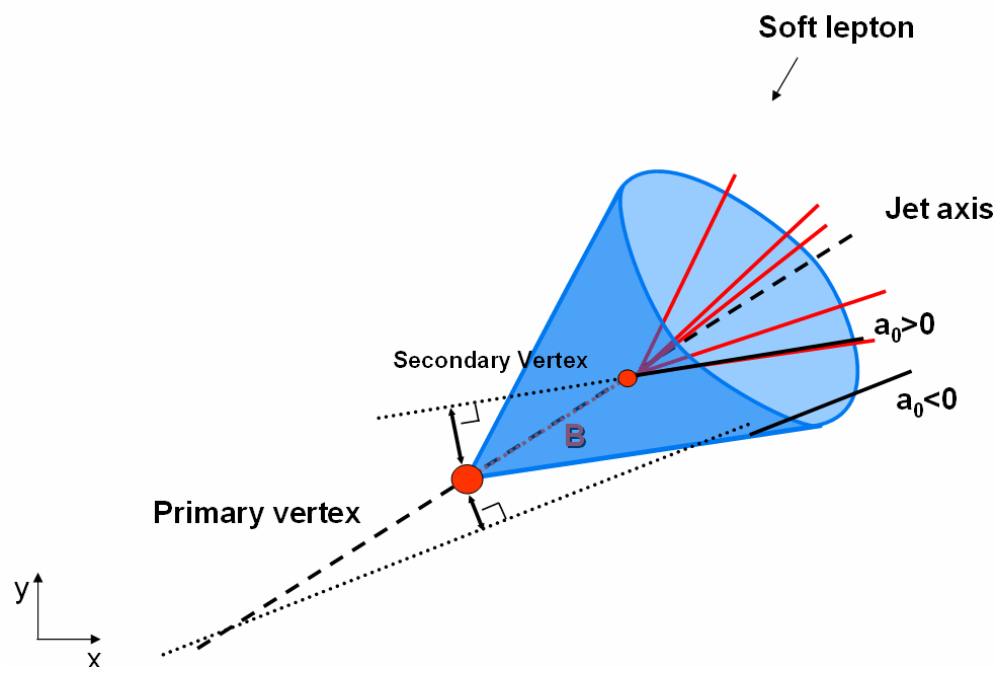

Impact parameter resolution (simplified)

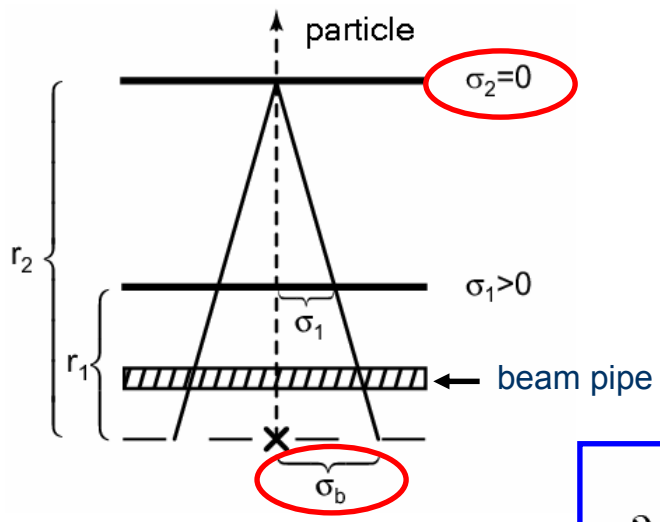

$$\frac{\sigma_b}{\sigma_1} = \frac{r_2}{r_2 - r_1}$$

small !

small !

$$\sigma^2 = \left(\frac{r_1}{r_2 - r_1}\,\sigma_2\right)^2 + \left(\frac{r_2}{r_2 - r_1}\,\sigma_1\right)^2 + \sigma_{MS}^2$$

small x/X_0

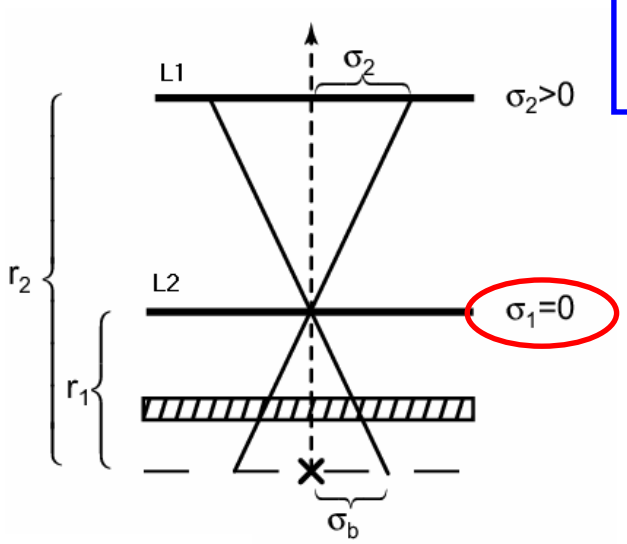

$$\frac{\sigma_b}{\sigma_2} = \frac{r_1}{r_2 - r_1}$$

$$\sigma_{MS} \sim \frac{1}{p}\sqrt{\frac{x}{X_0}}$$

… and … vertexing at LHC

pp → ttH (m=120 GeV)
H → bb
tt → W(lvl)b W(qq)b

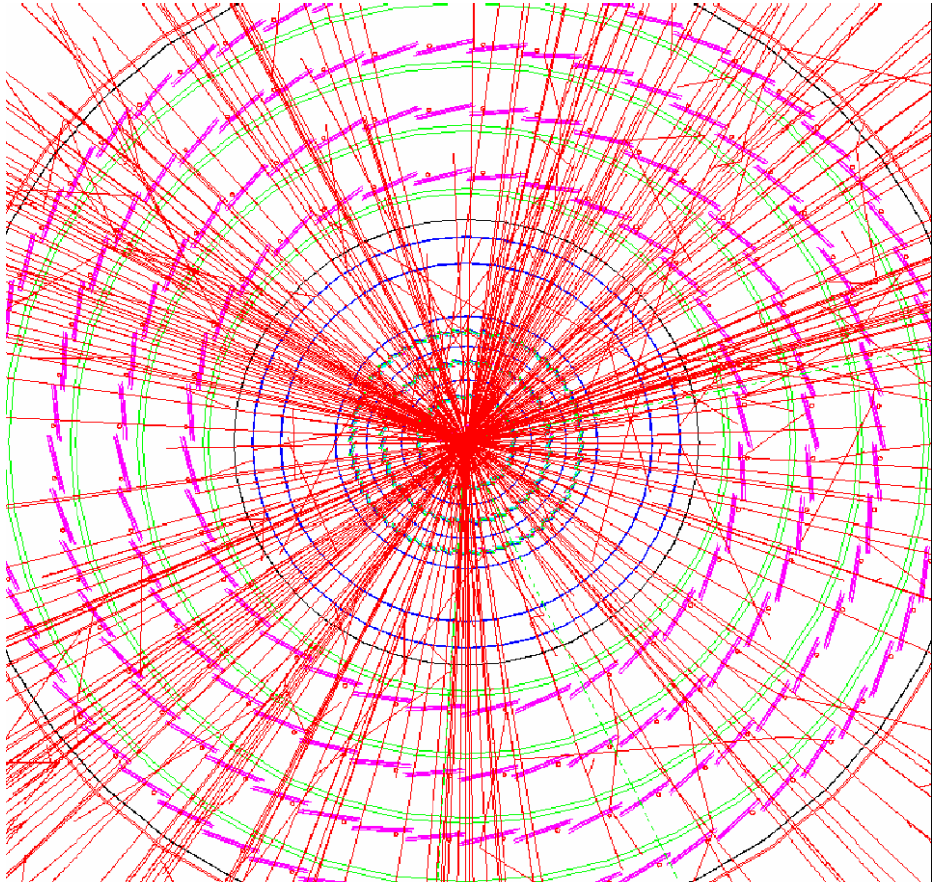

~ 1200 tracks/BX

high track density
in particular in jets

3D hit information
mandatory

pixels

10. Semiconductor Detectors: Charge Carriers

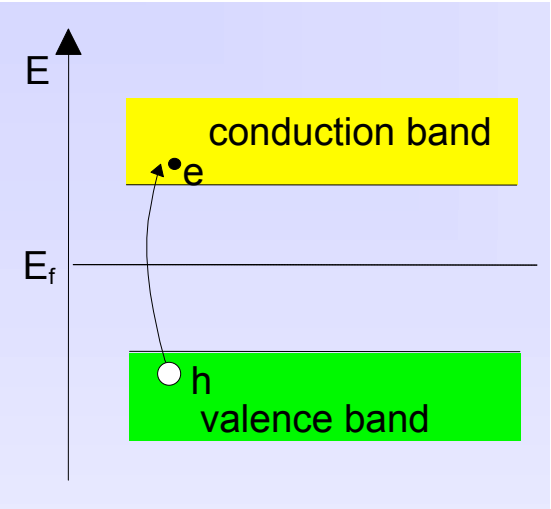

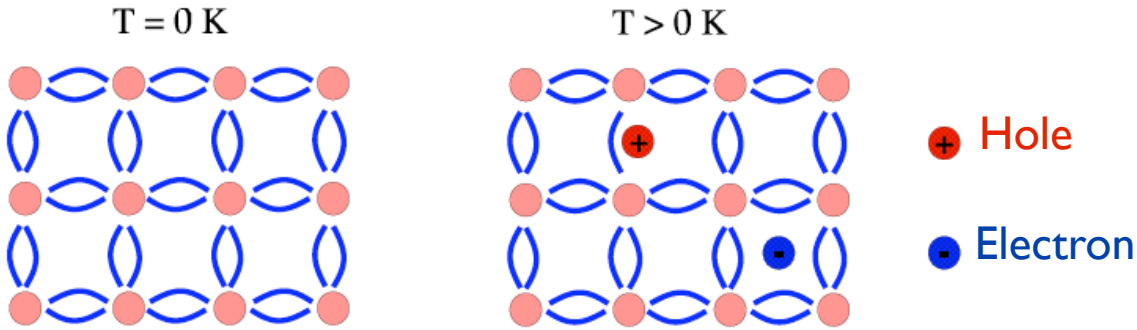

Silicon and germanium have 4 valence electrons, thus four covalent bounds. Thermal excitation excites electrons to the conduction band, which creates holes in the valence band.

Intrinsic electron(hole) concentration: $n_i = A\,T^{3/2}\ \exp(-E_g/2kT)$

(Si: Energy gap E_g = 1.12 eV, Ge: E_g=0.66 eV, T=20 ^{0}C ⇒ kT=1/40 eV)

Typical values at T = 300 K (compare to silicon concentration of 5×10^{22} cm^{-3})

Si: $n_i = 1.5 \times 10^{10}$ cm^{-3}

Ge: $n_i = 2.5 \times 10^{13}$ cm^{-3}

10. Signal from Ionizing Particle

Comparison for T=300 K and a pure Si volume shown on the right.

4.5×10^8 intrinsic e-h pairs

3.2×10^4 e-h pairs produced by M.I.P. (minimal ionizing particle)

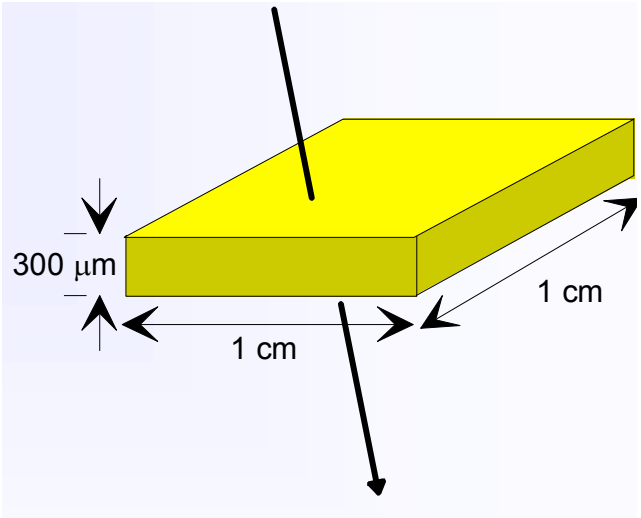

Conclusion:
Signal too small. Need to reduce free charge carriers, i.e. deplete the detector.

Use doped semiconductors to create reversed bias depleted p-n junction.

10. Doped Semiconductors (1)

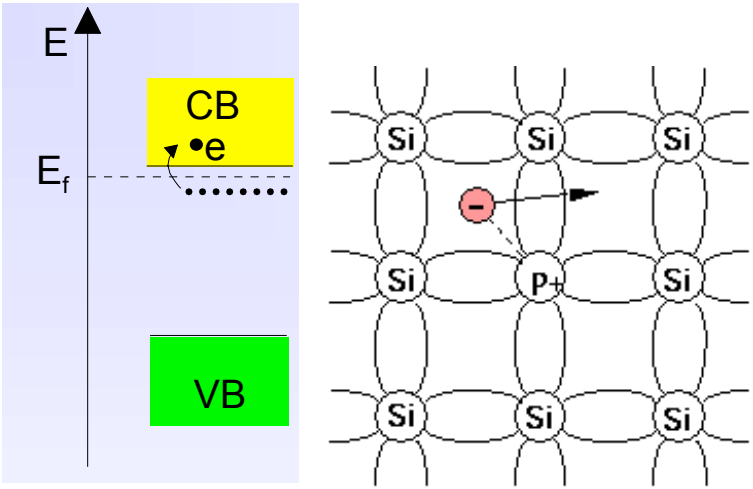

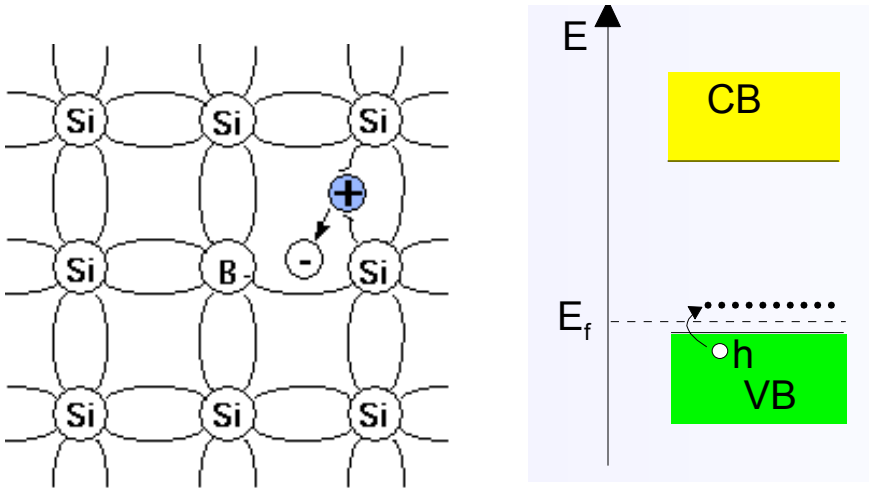

n-type silicon

- Si has 4 valence electrons
- add elements from Vth group (5 valence electrons)
- donors (phosphorous, arsenic) give away one electron.
- creates high energy level of electrons
- small thermal excitation (0.05 eV for Si) needed to increases electron concentration in CB.
- n-type: electron concentration n larger then hole concentration p.

  $n \cong N_D$ (N_D = donor concentration)

p-type silicon

- Si has 4 valence electrons
- add elements from III-rd group (3 valence electrons)
- acceptors (boron, Indium, gallium...) misses one electron
- creates discrete energy level for holes
- small thermal excitation needed to increases hole concentration in VB.
- p-type: holes are the majority carriers.

  $p \cong N_A$ (N_A = acceptor concentration)

10. Doped Semiconductors (2)

Typically one uses a very small concentration of dopants.

Silicon concentration: 5×10^{22} atoms/cm^3

Typical dopant concentration: 5×10^{13} atoms/cm^3

Heavily doped material used for electrical contacts (indicated with +), p+, n+ can be as high as 10^{20} atoms/cm^3 .

	detector grade	electronics grade
doping	$\approx 10^{12}$ cm^{-3}	$\approx 10^{17}$ cm^{-3}
resistivity ρ	$\approx$ 5 kΩ·cm	$\approx$1 Ω·cm

Conductivity

Two basic relations: $np = n_i^2 = AT^3 exp(-E_g/kT)$ with n_i = intrinsic carrier concentration

$N_D + p = N_A + n$ with N_D, N_A donor/acceptor concentrations

Example: n-type (e.g. N_A=0, n≫p) ; analogous result for p-type

majority carrier concentration $n \simeq N_D$,

minority carrier concentration $p=(n_i)^2/N_D$

Conductivity: $\sigma=1/\rho \simeq e\, N_D\, \mu_e$

μ_e : electron mobility

10. pn-junction

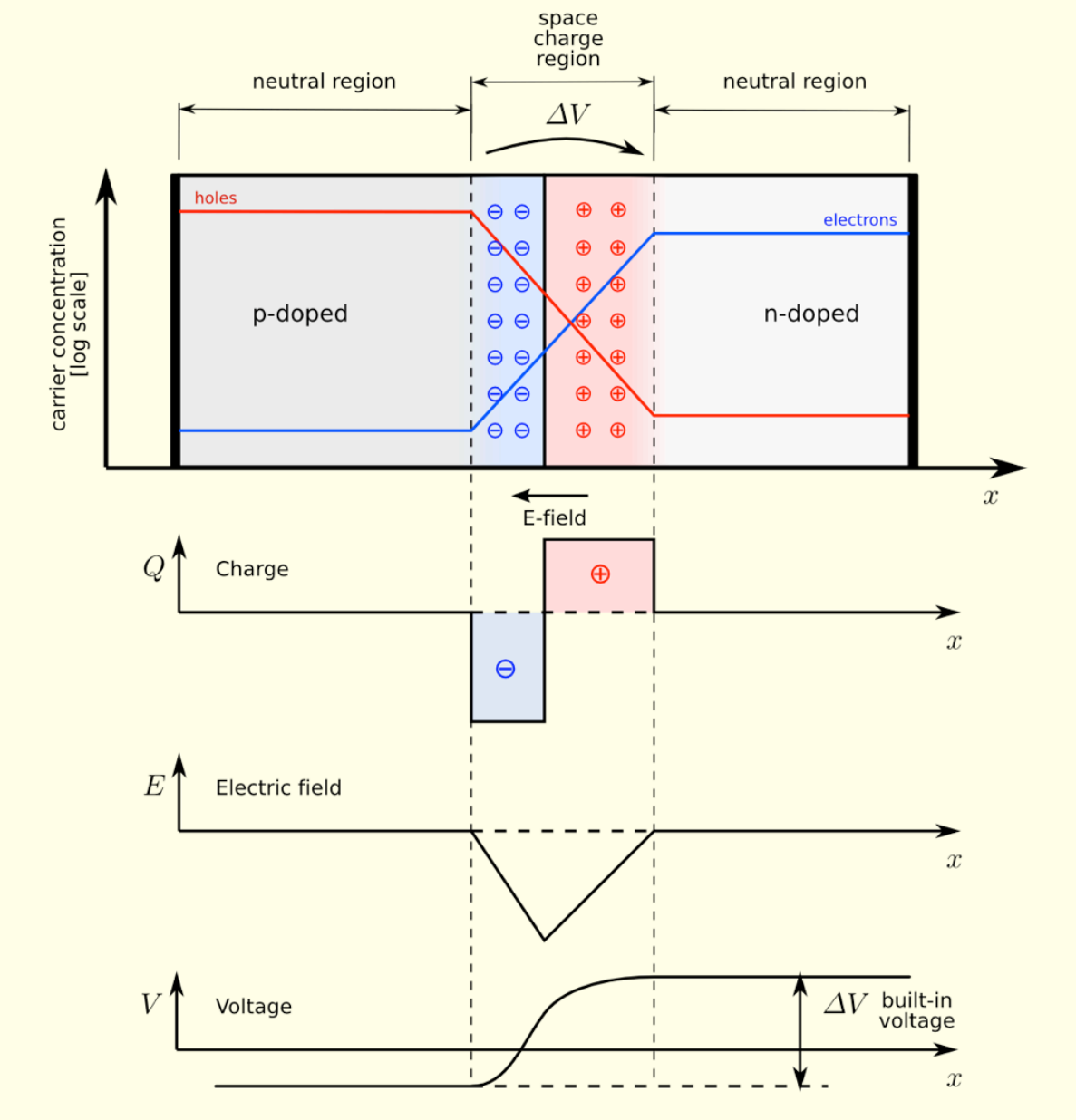

- p-type and n-type regions are neutral
- Electrons diffuse towards p-type and fill holes (recombination).
- Holes drift towards n-type
- Space charge builds up "-" on p-type and "+" on n-type.
- Space charge creates E-field.
- Potential difference exists at junction (contact potential, about 1 Volt).
- Space charge region is depletion zone (devoid of charge carriers). Any e-hole, which is created, will be swept away by the E-field.

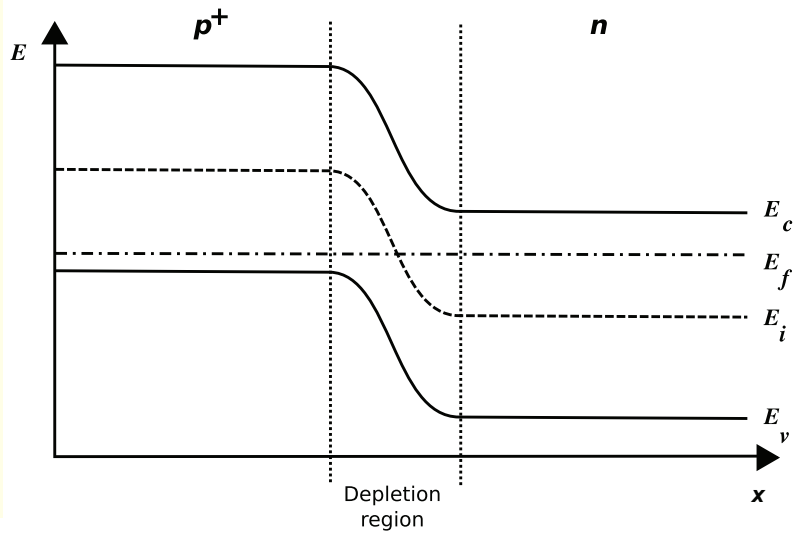

10. Depletion Width (1)

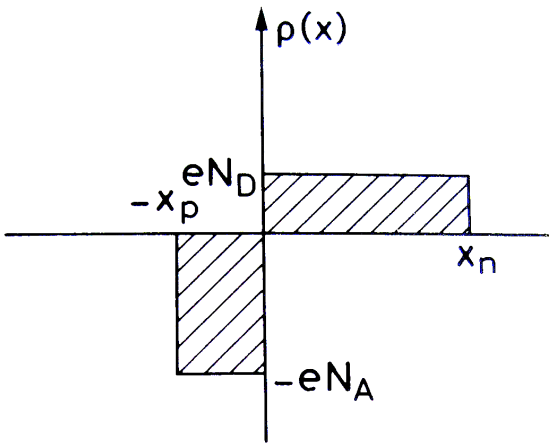

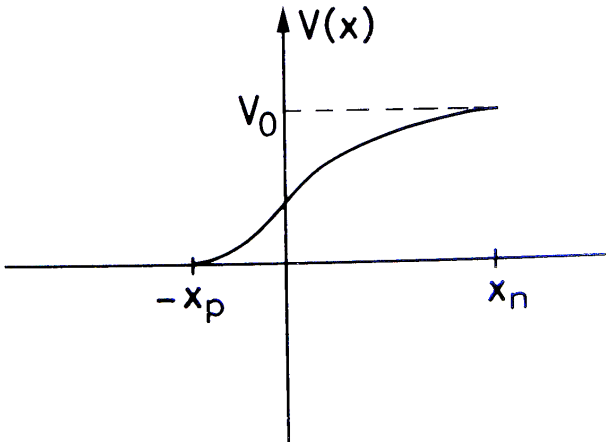

Total charge is conserved: $N_A x_p = N_D x_n$

high p doping ($N_A \gg N_D$): $x_n \gg x_p$

high n doping ($N_D \gg N_A$): $x_p \gg x_n$

Depletion is mainly in lower doped region

Solution of Poisson equation:

$$x_n = \sqrt{\frac{2\epsilon\epsilon_0 V_0}{e}\frac{N_A}{N_D(N_A+N_D)}}$$

$$x_p = \sqrt{\frac{2\epsilon\epsilon_0 V_0}{e}\frac{N_D}{N_A(N_A+N_D)}}$$

Depletion width w:

$$w = x_n + x_p = \sqrt{\frac{2\epsilon\epsilon_0 V_0}{e}\left(\frac{1}{N_D}+\frac{1}{N_A}\right)}$$

Built-in voltage V :

$$V_0 = \frac{kT}{e}\ln\frac{N_A N_D}{n_i^2}$$

Example: Silicon pn-junction at room temperature with $N_A=10^{16}$ cm^{-3}, $N_D=10^{12}$cm^{-3} gives V_0=0.458 V

10. Depletion Width (2)

For the typical case of very asymmetric doping, i.e. $N_A \gg N_D$, one gets with

$$w = x_n + x_p = \sqrt{\frac{2\epsilon\epsilon_0 V_0}{e}\left(\frac{1}{N_D} + \frac{1}{N_A}\right)} \quad \text{and} \quad x_n = \sqrt{\frac{2\epsilon\epsilon_0 V_0}{e}\frac{N_A}{N_D(N_A + N_D)}}$$

Depletion width $$w \simeq x_n \simeq \sqrt{\frac{2\epsilon\epsilon_0 V_0}{eN_D}}$$

Other formulae:

Max. E-Field at junction: $$E_{max} = \frac{1}{\epsilon\epsilon_0} eN_D x_n = \frac{1}{\epsilon\epsilon_0} eN_A x_p \simeq \sqrt{\frac{2e}{\epsilon\epsilon_0} N_D V_0}$$

Example:

Silicon pn-junction at room temperature with, $N_A=10^{16}$ cm^{-3}, $N_D=10^{12}$cm^{-3} , $V_0=0.458$ V

W = 25 µm and E_{max} = 384 V/cm

10. Reversed Bias Voltage

Increase depletion width with reversed bias

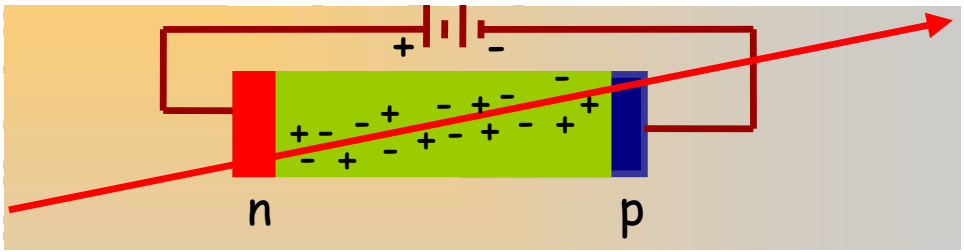

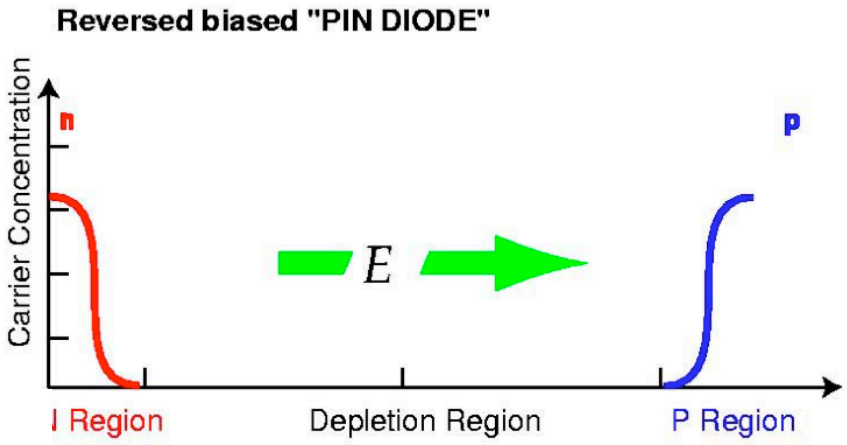

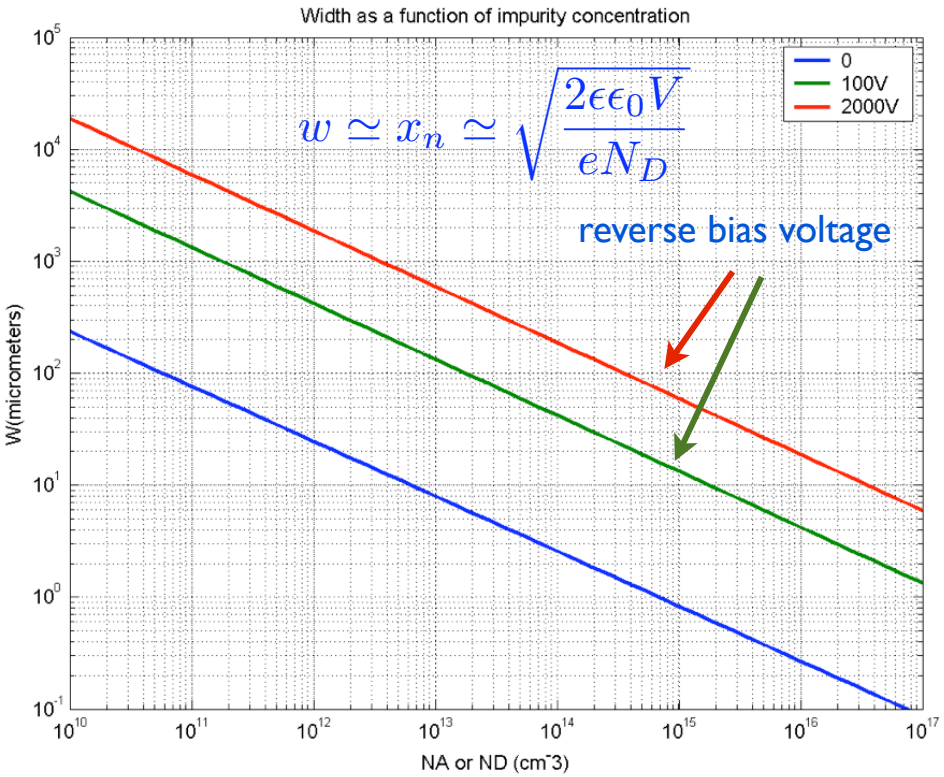

Electron - hole pairs,
created in the depletion region
by the ionizing particle,
drift in the electric field.

typical ionization: 100 e-h pairs/μm
typical noise: 1000 electrons

Large S/N requires large depletion region, i.e.
large reverse bias voltage.

11. Silicon Strip Detector

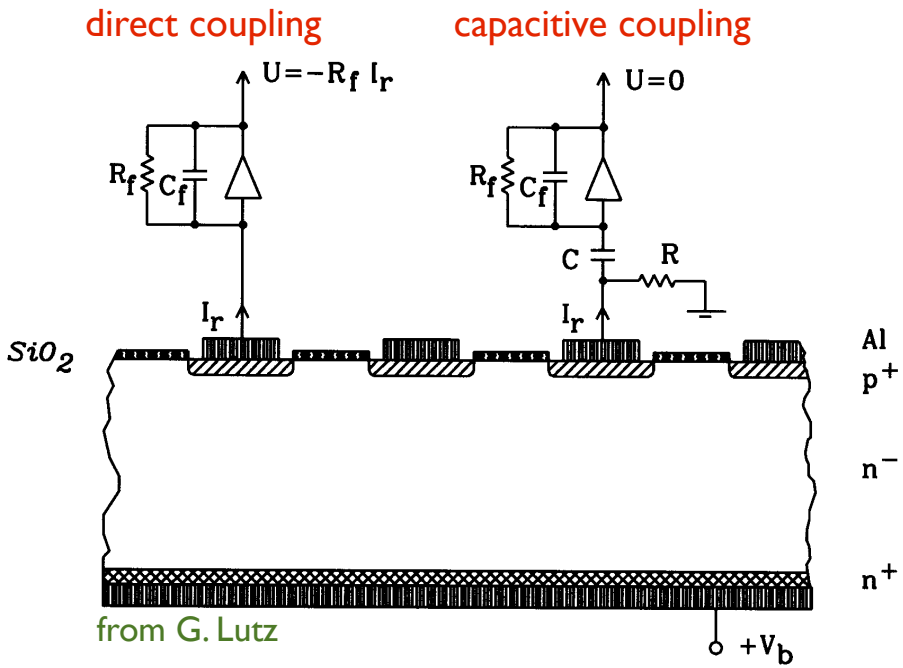

from G. Lutz

Direct coupling: reverse current I_r is absorbed by electronics.

Capacitive coupling: AC part goes to amplifier,
DC part goes through bias resistor R.

Typical detector thickness: 300 µm (150µm - 500 µm)

Typical strip separation, pitch p: 20 µm - 150 µm

Position resolution: $\sigma = p / \sqrt{12} \simeq 14$ µm (p=50 µm)

- Bias resistor produced by deposition of polysilicon.
- Capacitors produced via metal readout lines over implants (S_iO_2 isolation).

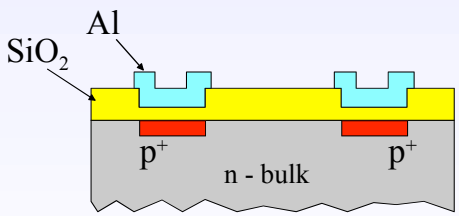

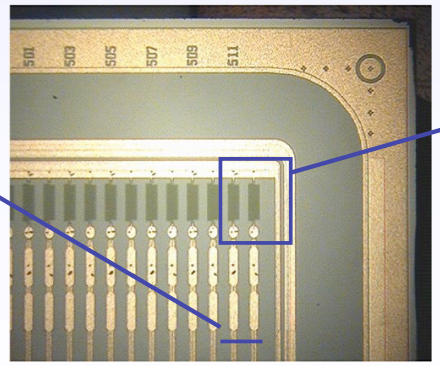

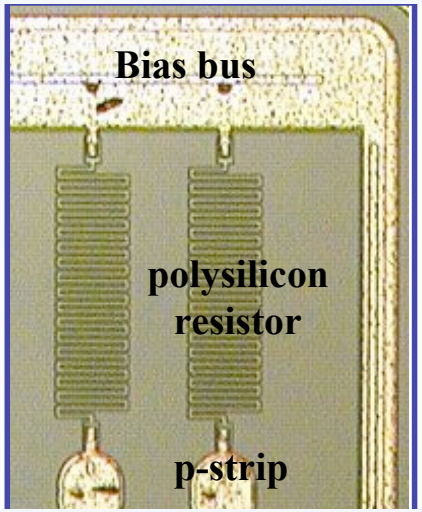

Several different methods are used to readout strips and to provide bias voltage. They are implemented in the manufacturing process.

11. Example: n-strip and p-stop

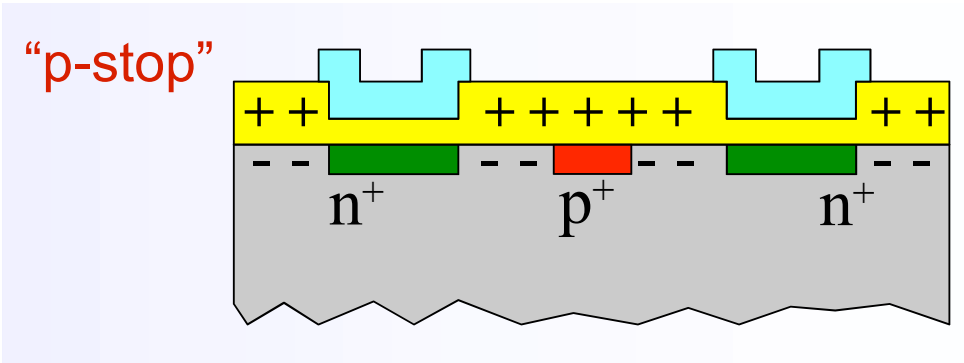

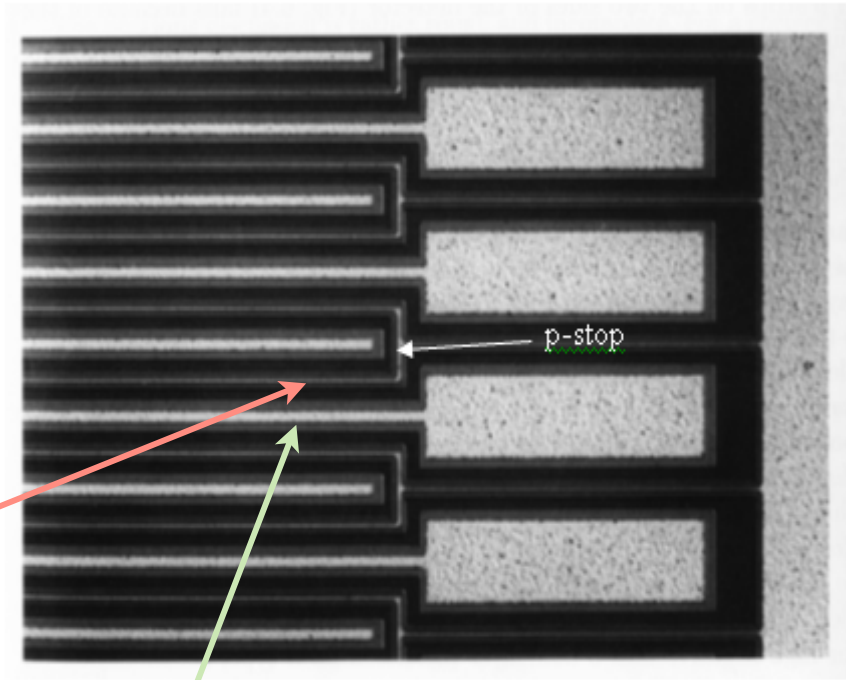

p-stop

n-strip

11. Measured Signal

Collected Charge for a Minimum Ionizing Particle (MIP)

- **Mean energy loss**
  dE/dx (Si) = 3.88 MeV/cm
  ⇒ 116 keV for 300μm thickness

- **Most probable energy loss**
  ≈ 0.7 ×mean
  ⇒ 81 keV

- **3.6 eV to create an e-h pair**
  ⇒ 72 e-h / μm (mean)
  ⇒ 108 e-h / μm (most probable)

- **Most probable charge** (300 μm)

  ≈ 22500 e ≈ 3.6 fC

Most probable charge ≈ 0.7× mean

Mean charge

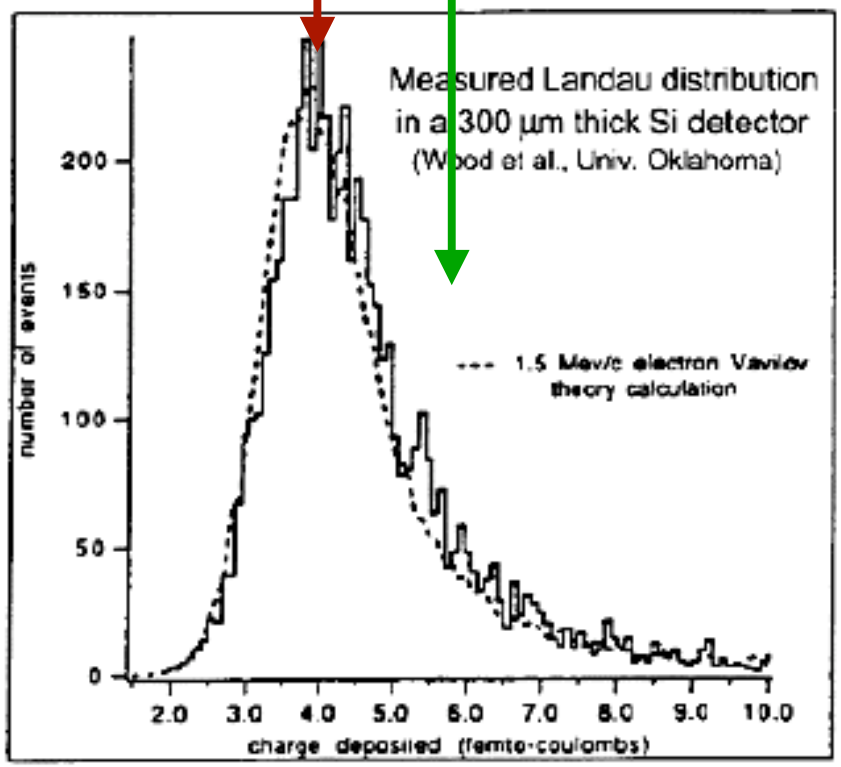

from M. Moll

11. Signal to Noise ratio (S/N)

- **Landau distribution** has a low energy tail
  - becomes even lower by noise broadening

Noise sources: (ENC = Equivalent Noise Charge)

- Capacitance $ENC \propto C_d$
- Leakage Current $ENC \propto \sqrt{I}$
- Thermal Noise (bias resistor) $ENC \propto \sqrt{k_B T / R}$

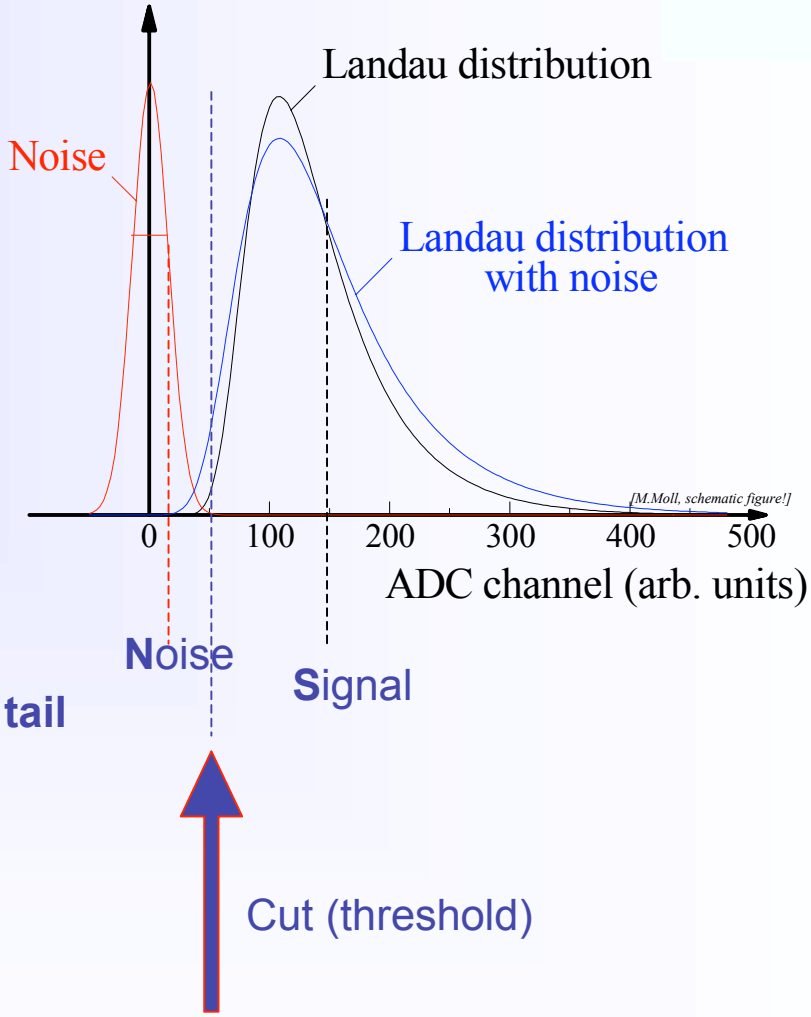

- **Good hits selected by requiring N_{ADC} > noise tail**
  If cut too high ⇒ efficiency loss
  If cut too low ⇒ noise occupancy
- **Figure of Merit: Signal-to-Noise Ratio S/N**
- **Typical values >10-15, people get nervous below 10.**
  Radiation damage severely degrades the S/N.

from M. Moll

11. Signal Spread: Charge Collection and Diffusion

Charge collection time:

Drift velocity of charge carriers $v \simeq \mu E$ and drift time $t_d = d/v = d/\mu E$.

Typical values: d=300 μm, E=2.5 kV/cm (μ_e=1350 cm^2/Vs and μ_h=450 cm^2/Vs).

Drift times: $t_d(e)$ = 9 ns, $t_d(h)$ = 27 ns

Diffusion:

Diffusion of charge cloud caused by scattering of charge carriers. Width of distribution increases with drift time t_d. Using the diffusion constant $D = \mu kT/e$ one finds:

$$\sigma = \sqrt{2Dt_d} = \sqrt{\frac{2dkT}{eE}}$$

Note that diffusion is the same for electrons and holes, since the mobility drops out.

Typical charge width: 8-10 μm in 300 μm thick silicon. Width of charge cloud could be exploited to obtain better position resolution due to charge sharing between strips (charge centroid finding).

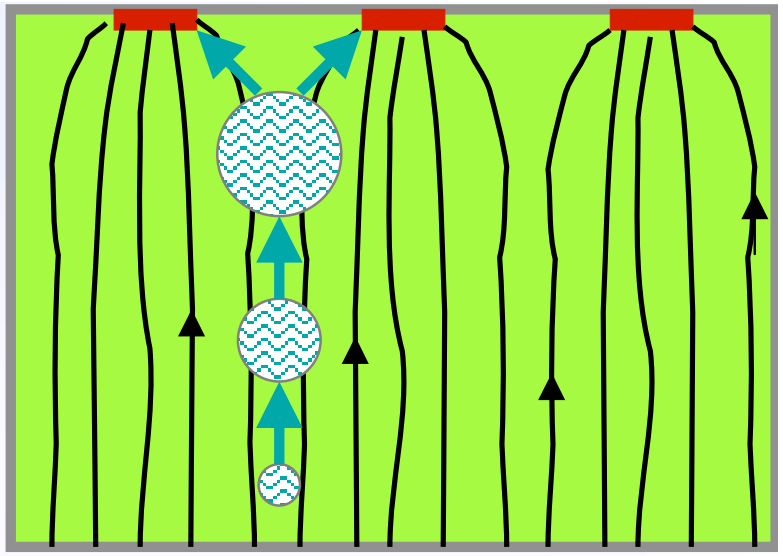

from M. Moll

11. Signal Spread: Lorentz Angle in B-field

N. Wermes

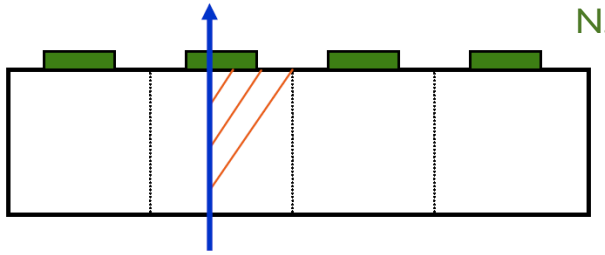

Lorentz angle

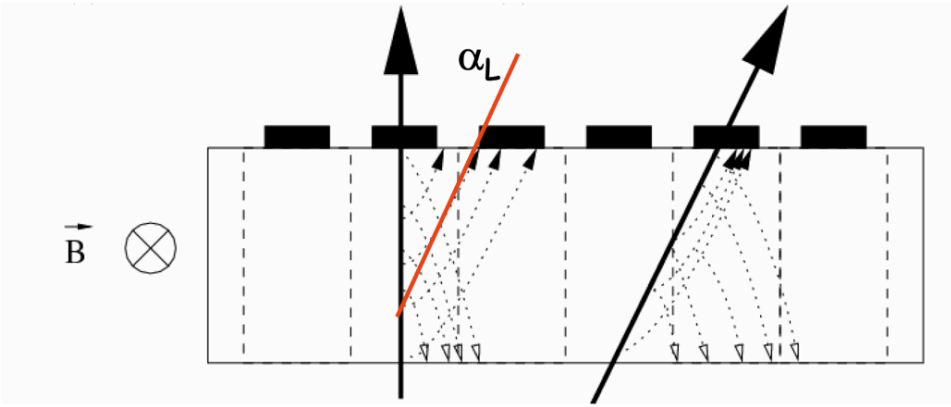

$$\tan \alpha_L = \mu_{Hall} B_\perp$$

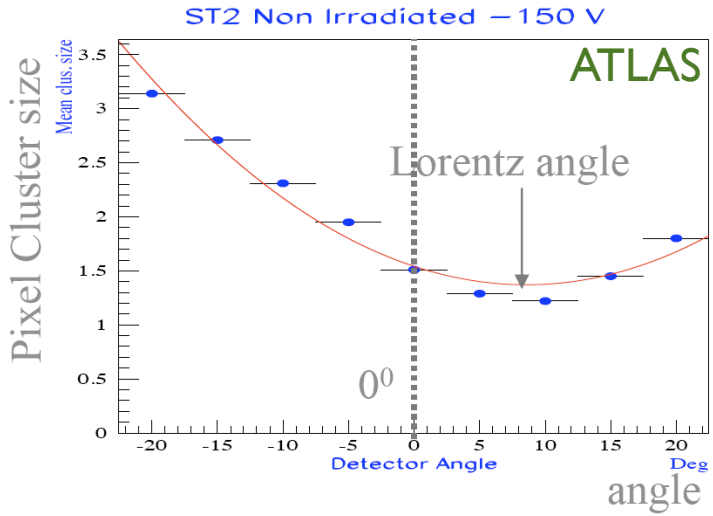

Measurement of Lorentz angle:

Number of strip (or pixel) hits is minimum, if incident angle of beam is equal to Lorentz angle.

Silicon detectors are built at a tilt angle to compensate for the Lorentz angle.

Effective incident angle = tilt angle + Lorentz angle

11. Detector Module: ATLAS Endcap SCT

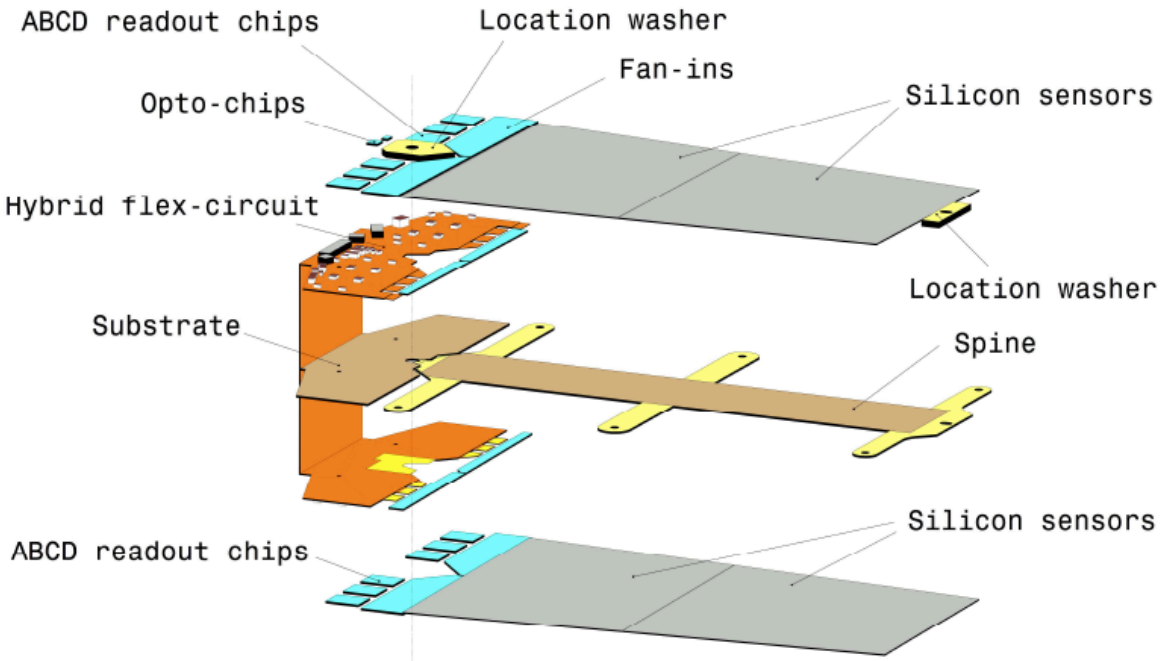

ATLAS Silicon central tracker SCT

Endcap:
1976 modules with 2 sensors glued back to back on spine.

Rotation by 20 mrad (Rφ resolution)

Spine conducts heat.

Alignment position of sensors ≃2 μm.

Strip pitch 80 μm, width 12 μm.

Resolution 16 μm in R-φ.

Operation temperature -7 °C.

99.8% of strips are working.

11. Wire Bonding

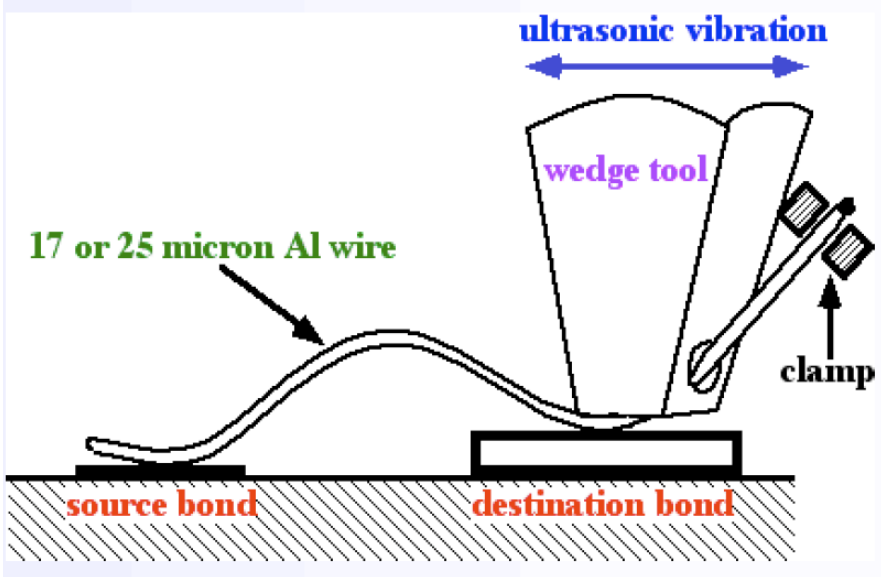

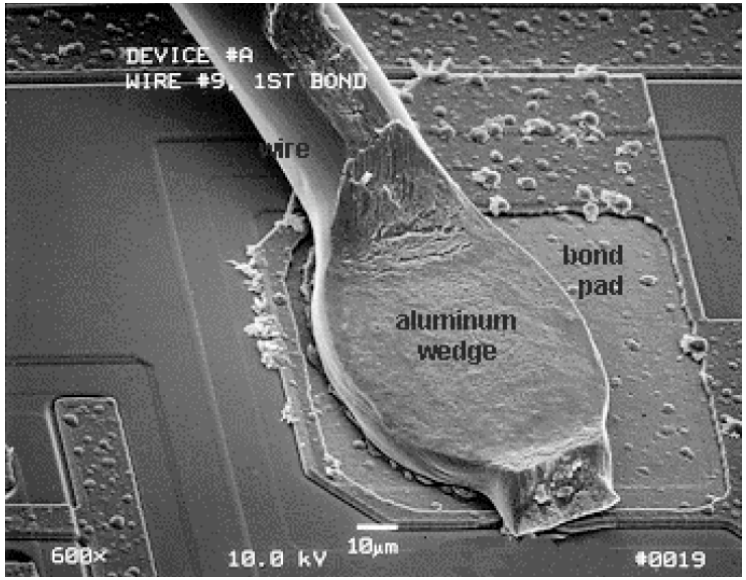

Bond foot picture (electron microscope)

Ultrasonic excitation causes vibration of needle.
Friction heat welds 25 µm Al wire to metal pad.

Bonding is heavily used in industry, PC processors, but with thicker wires and larger pitch.

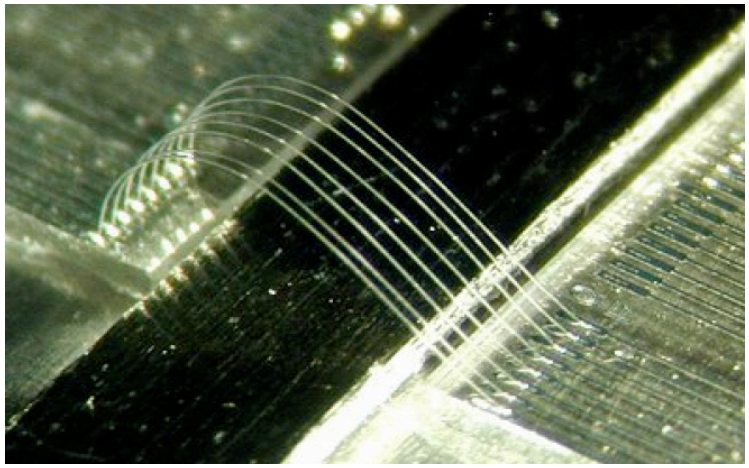

Connection of sensor to electronics (microscope)

11. Connection to electronics

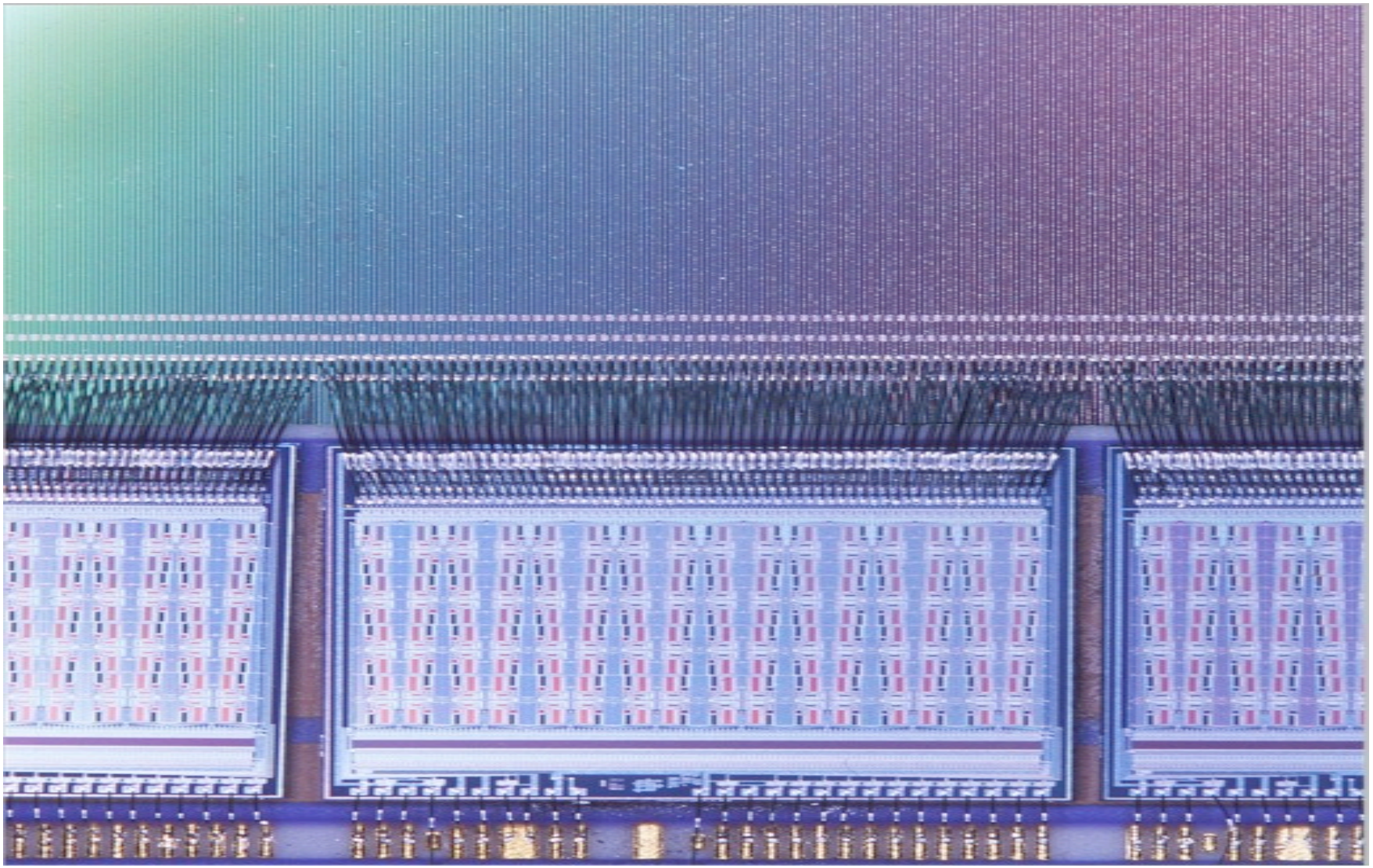

ASICS

11. Hybrid Active Pixel Detector

- **HAPS – Hybrid Active Pixel Sensors**
  - segment silicon to diode matrix with high granularity
    (⇒ true 2D, no reconstruction ambiguity)
  - readout electronic with same geometry
    (every cell connected to its own processing electronics)
  - connection by "bump bonding"
  - requires sophisticated readout architecture
  - Hybrid pixel detectors will be used in LHC experiments:
    ATLAS, ALICE, CMS and LHCb

Solder Bump: Pb-Sn

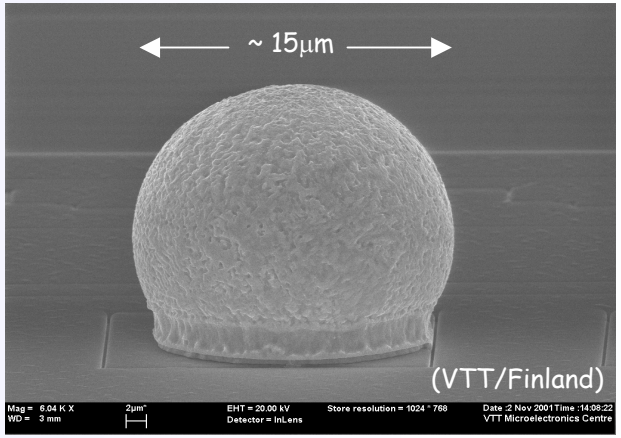

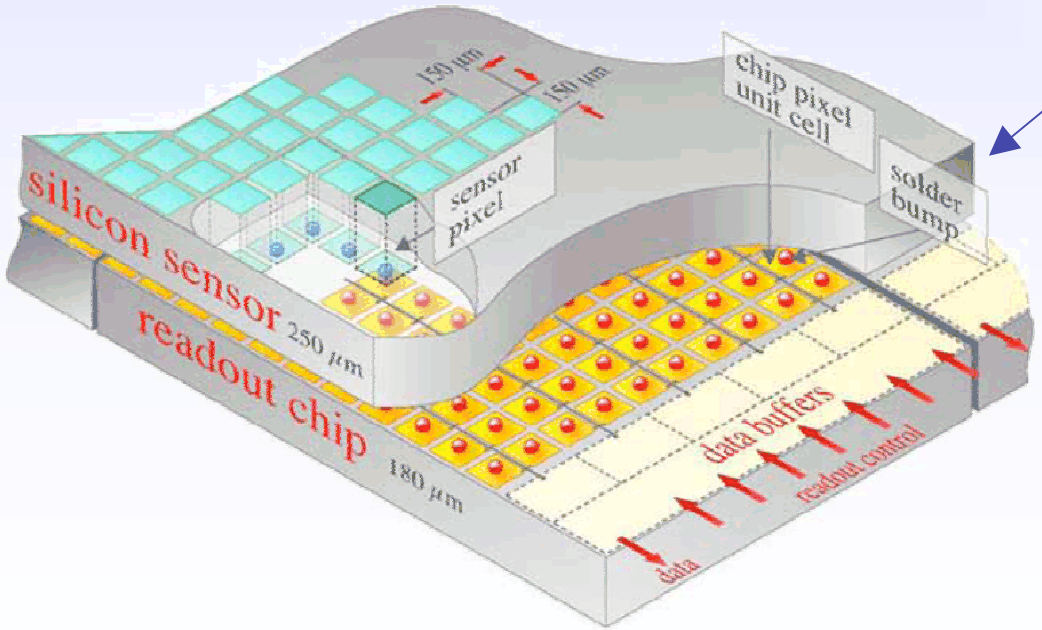

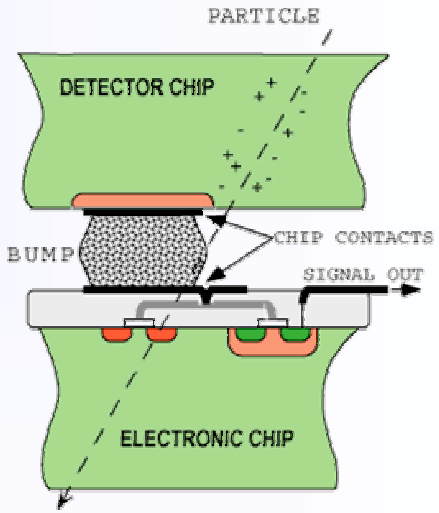

Flip-chip technique

from M. Moll

12. Radiation Damage: Radiation Levels at LHC and SLHC

Example: ATLAS

- Fluences per year at full Luminosity

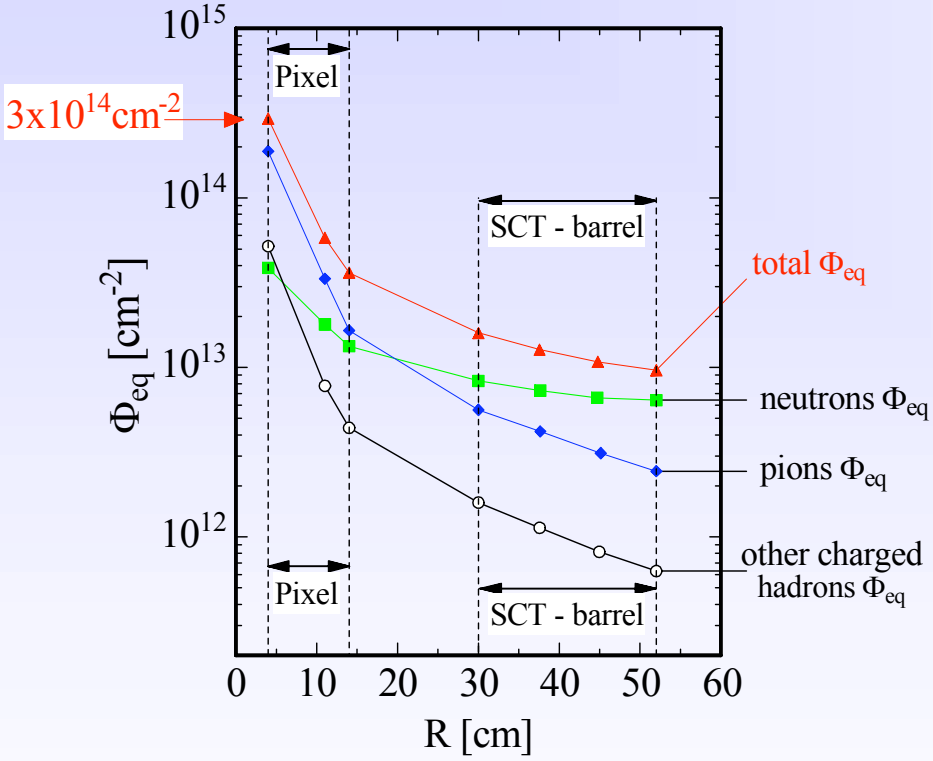

- Pixel detector: up to $\Phi_{eq} \approx 3.5 \cdot 10^{14}$ cm^{-2} /year
- Dominating type of particle is different for pixel (pions) and strip detectors (neutrons)

LHC silicon detectors:

- All detectors have been extensively tested and developed for radiation tolerance and are expected to survive the LHC radiation environment.
- Some experiments have already foreseen upgrades (e.g. LHCb Velo after 3 years).

Super LHC

- upgrade of LHC to 10 x higher Luminosity
  - ⇒ 10 x higher radiation levels
  - ⇒ Radiation damage will become a critical issue!
  - ⇒ New, radiation tolerant detectors needed!

- What is radiation damage ?
- How to cope with it ?

from M. Moll

12. Radiation Damage: Microscopic Defects

from M. Moll

- **Damage to the silicon crystal:** Displacement of lattice atoms

particle → Si_S —E_K>25 eV→ 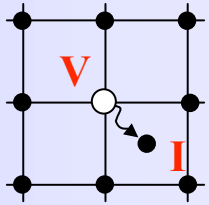

Vacancy + Interstitial ⇔ **"point defects", mobile in silicon, can react with impurities (O,C,..)**

E_K > 5 keV → **point defects and clusters of defects**

80 nm

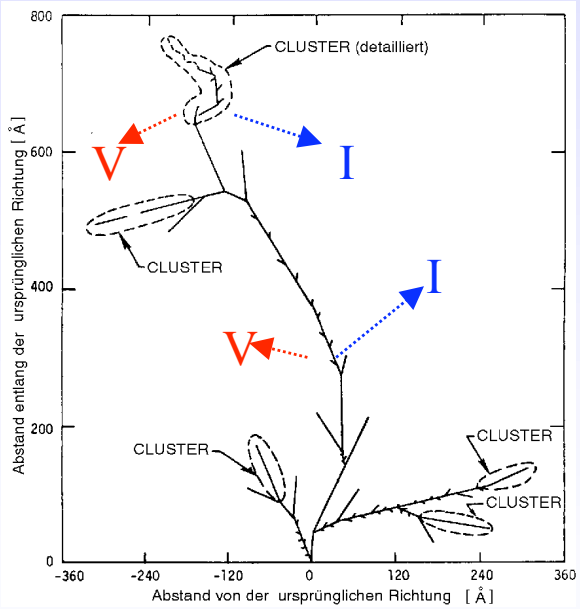

Distribution of vacancies created by a 50 keV Si-ion in silicon (typical recoil energy for 1 MeV neutrons):

← **Schematic** [Van Lint 1980]

Simulation → [M.Huhtinen 2001]

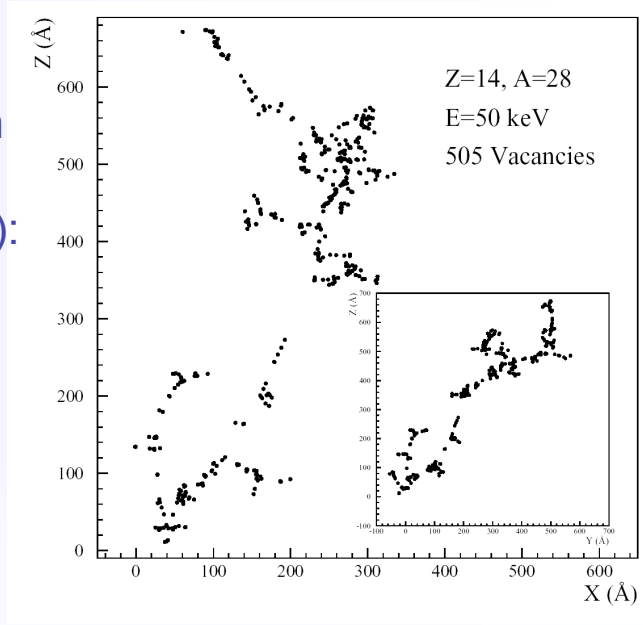

- **Defects can be electrically active (levels in the band gap)**
  - capture and release electrons and holes from conduction and valence band
  - ⇒ can be charged - can be generation/recombination centers - can be trapping centers

The CMS Experiment

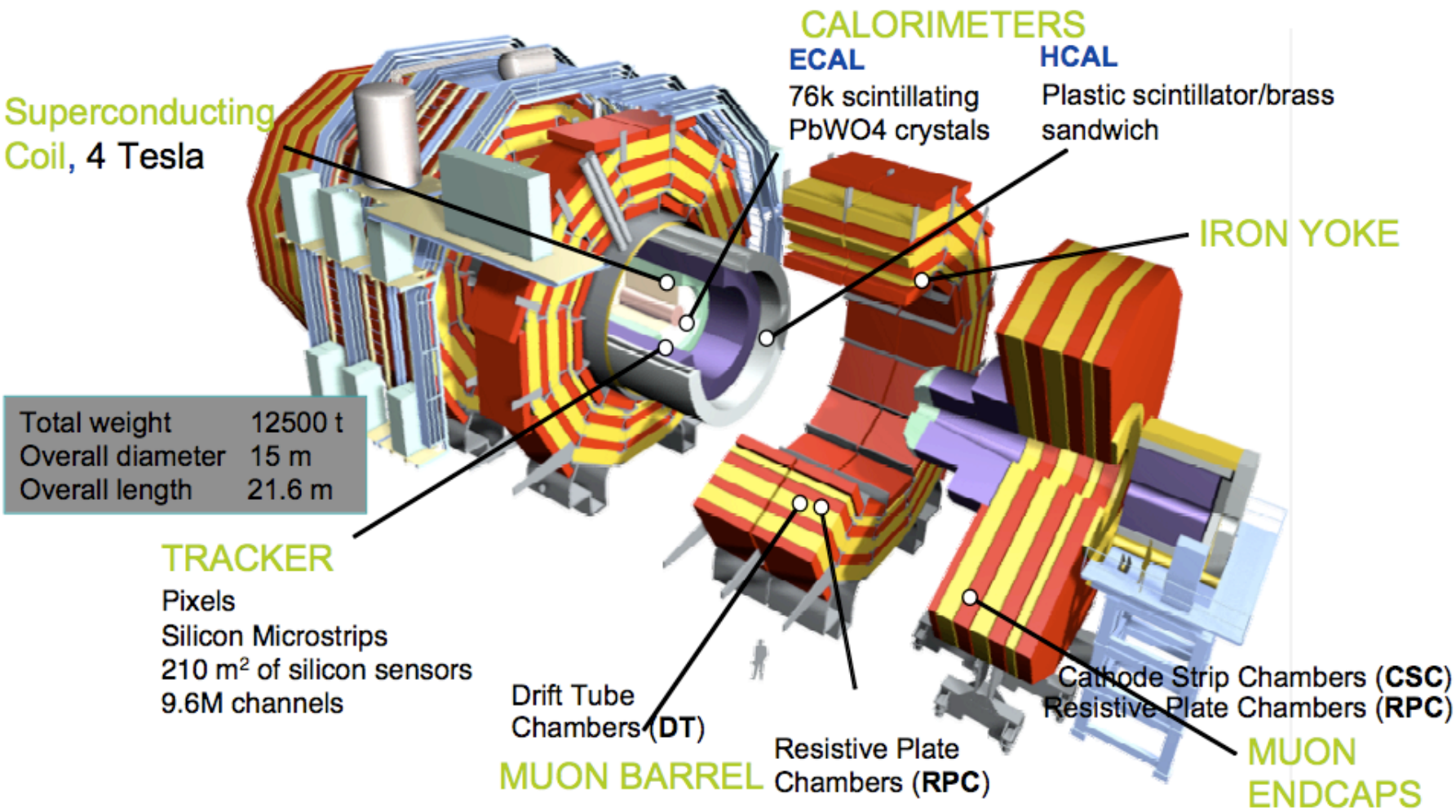

14. CMS Detector

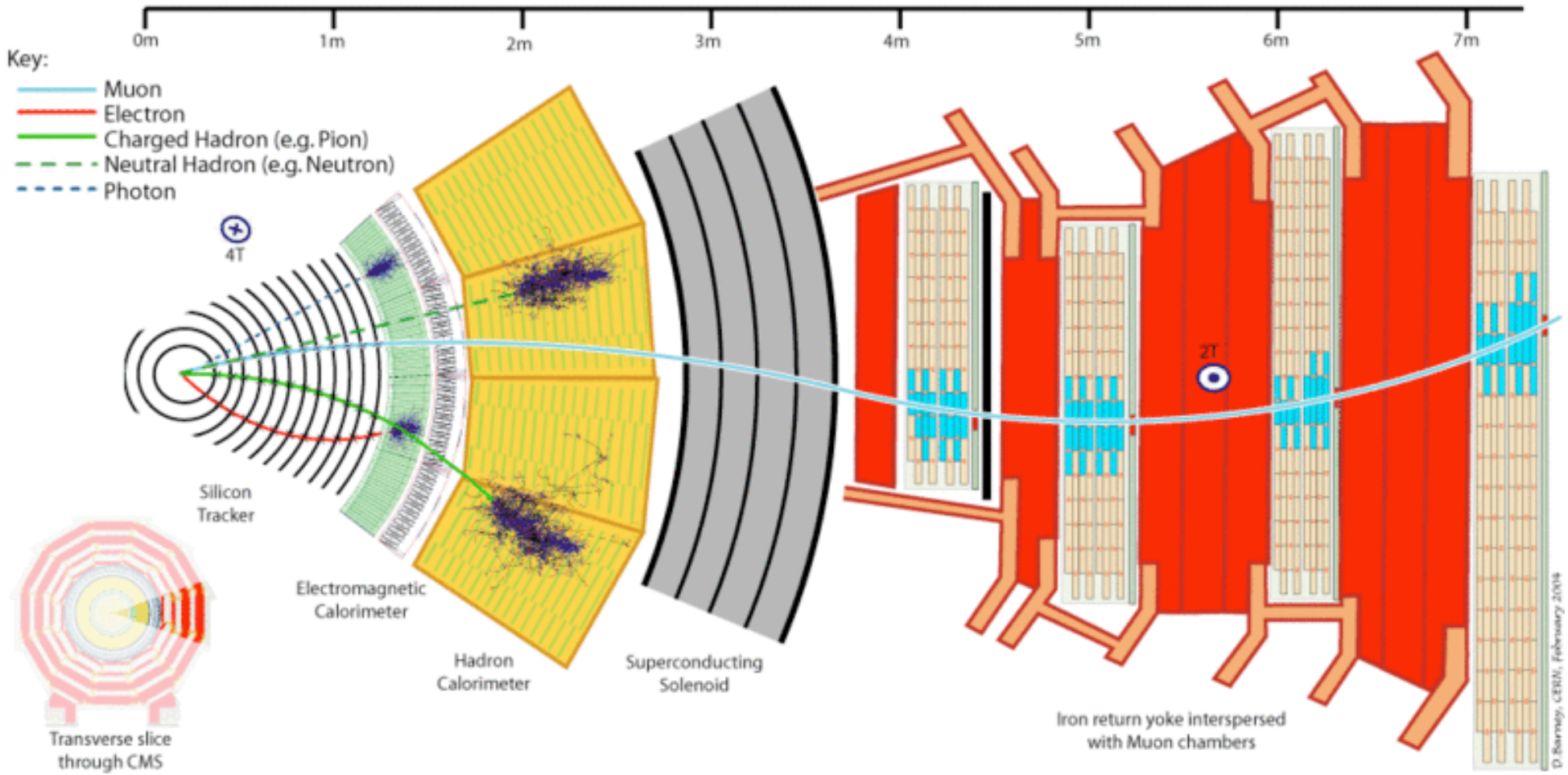

14. CMS Silicon Tracker

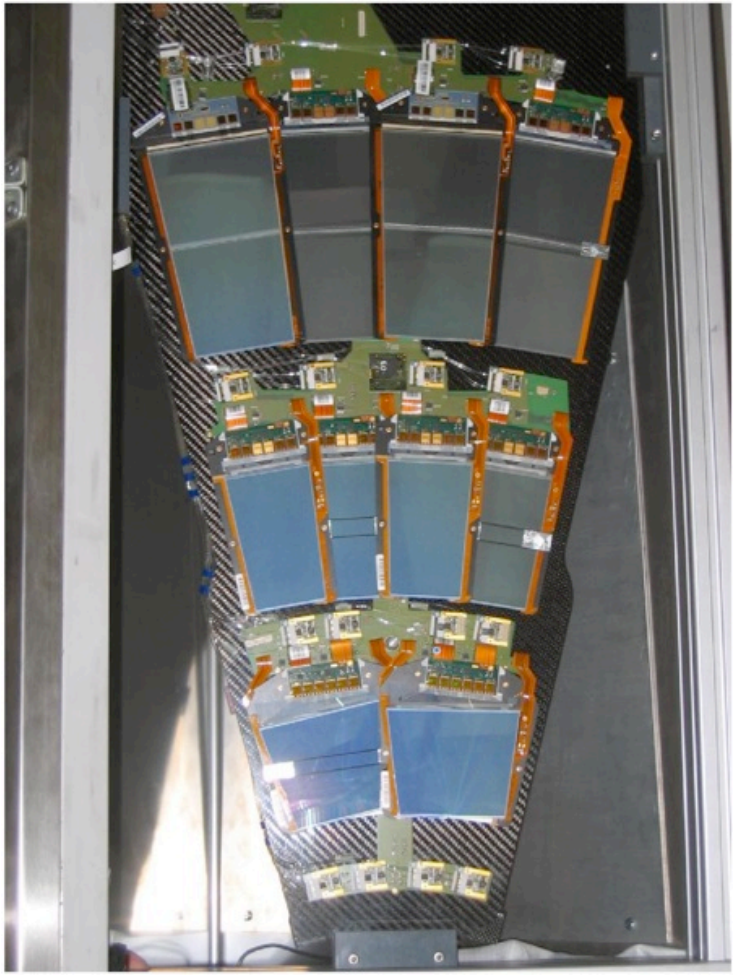

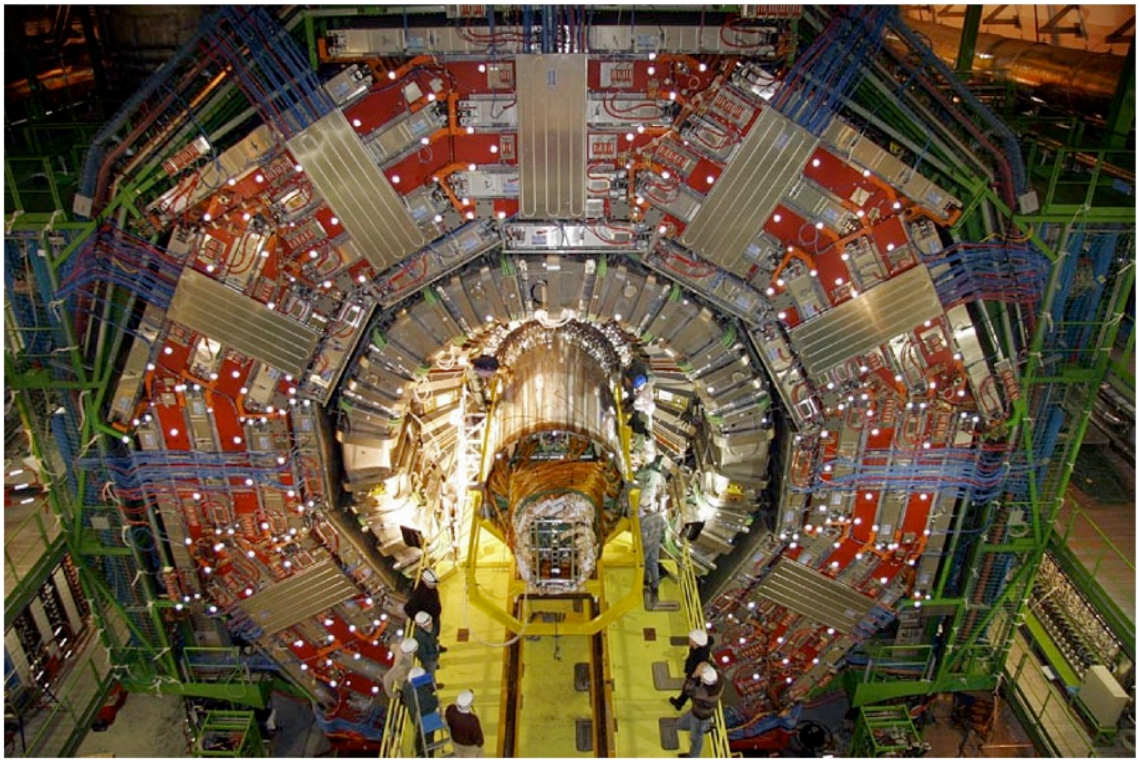

Micro Strip:

- 214 m^2 of silicon strip sensors
- 11.4 million strips
- Diameter: 2.4 m

Pixel:

- Inner 3 layers: silicon pixels (~ 1 m^2)
- 66 million pixels (100x150 μm^2)
- Precisio: $\sigma(r\varphi) \sim \sigma(z) \sim 15\ \mu m$

Event Display

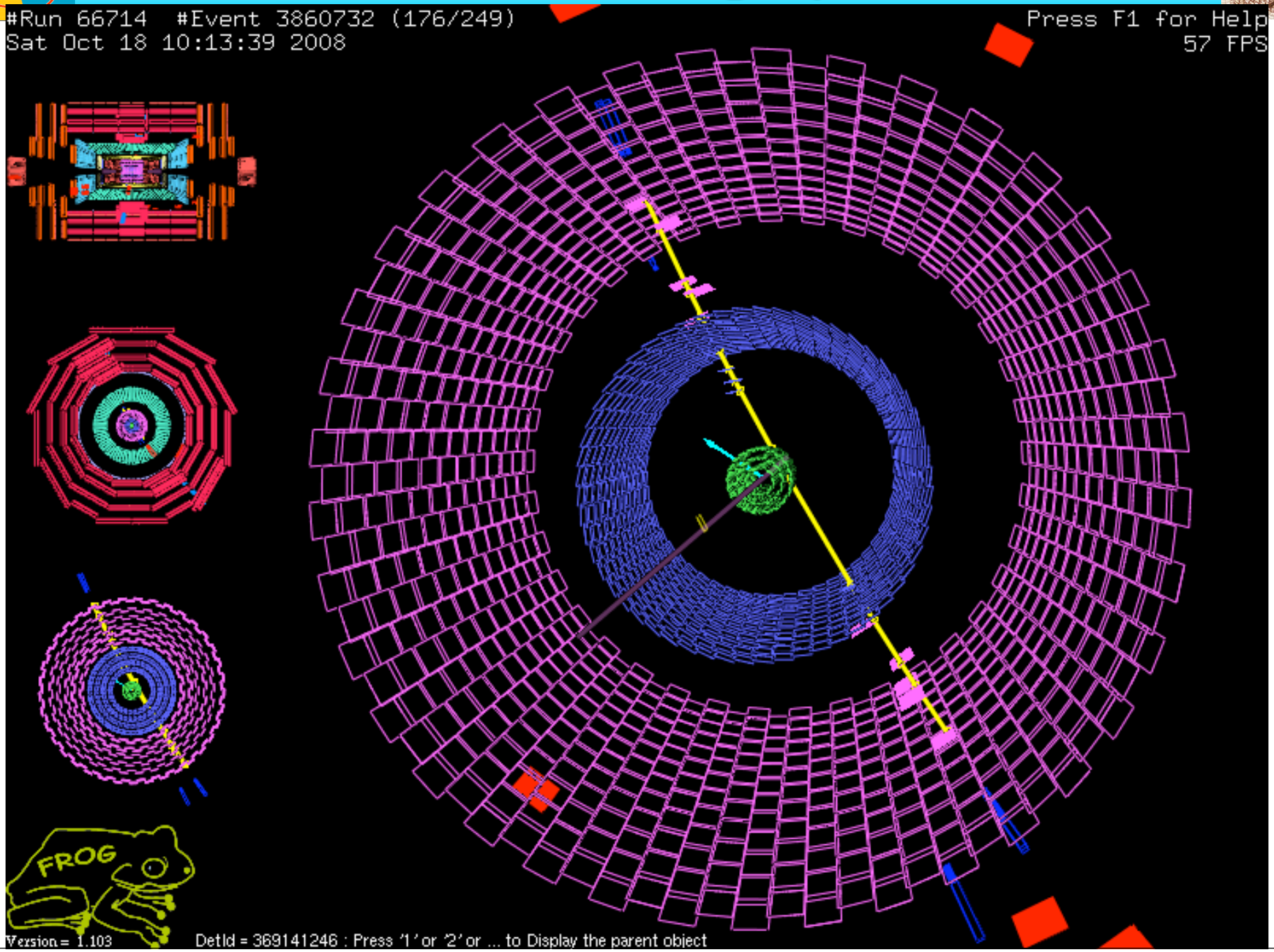

Tracker performance: Clusters

Signal-to-Noise ratio (S/N) for clusters associated to tracks. The track direction is used to correct the signal for the path length with respect to normal incidence

S/N value for TIB (320 um) and TOB (500 um): similar performance for thin and thick modules due to a different strip length: ~ 11 (~19) cm for TIB/TOB

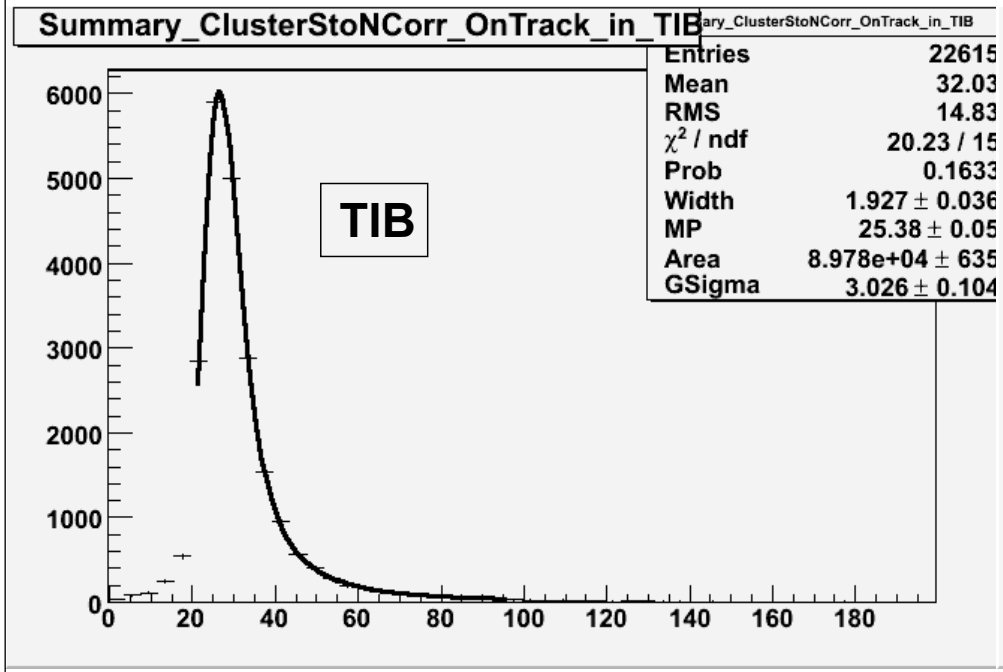

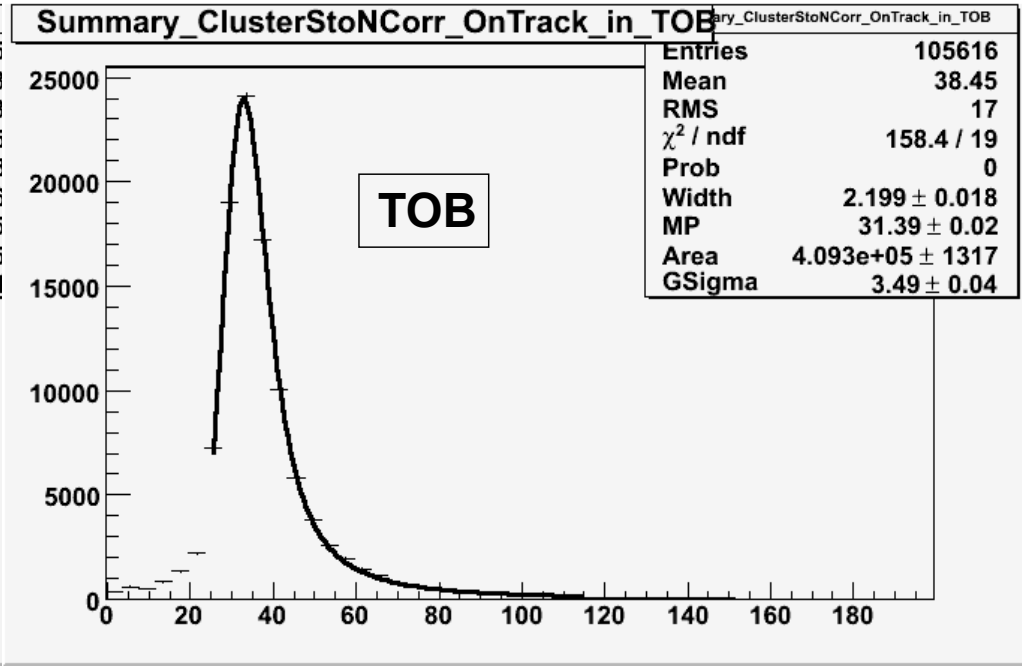

Most Probable Value (MPV) for each subsystem from the fit with a Landau function convoluted with a Gaussian
Value in agreement with expectation

	TIB	TOB	TID	TEC
S/N	25.4	31.4	27.5	30.4

Reconstruction efficiency

Collision-like inside-outside reconstruction

Standard LHC tracking algorithm (CTF) inside-outside with some modifications:

- a wider seeding ($p_T > 5$ GeV, $|d0| < 10$ cm)
- correct accounting of energy losses for tracks in the upper half

For cosmic tracks in the central region ($p_T > 10$ GeV, $|d0| < 10$ cm, $|dz| < 30$ cm; $10 \leq$ hits ≤ 25), use one track and check another reconstructed track opposite to it

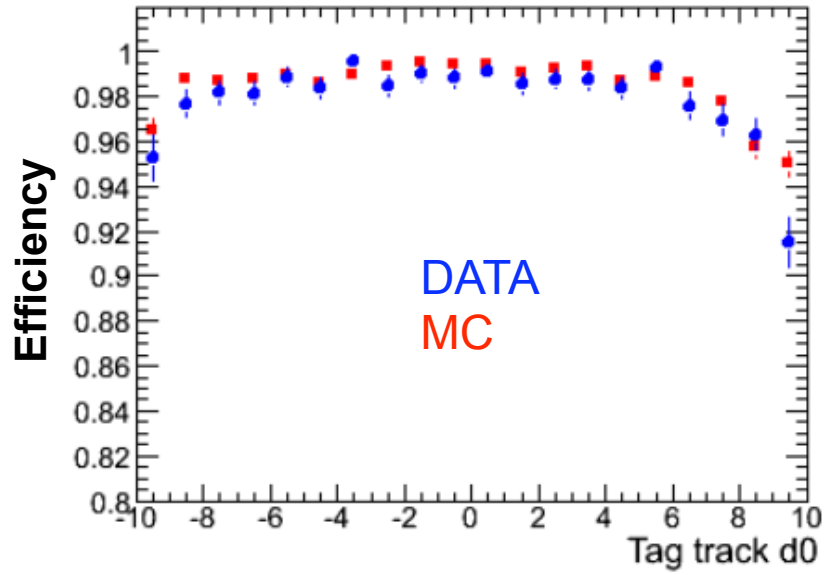

Results from cosmic data (in blue) are compared with MC events (in red)

High efficiency and good agreement between data and MC

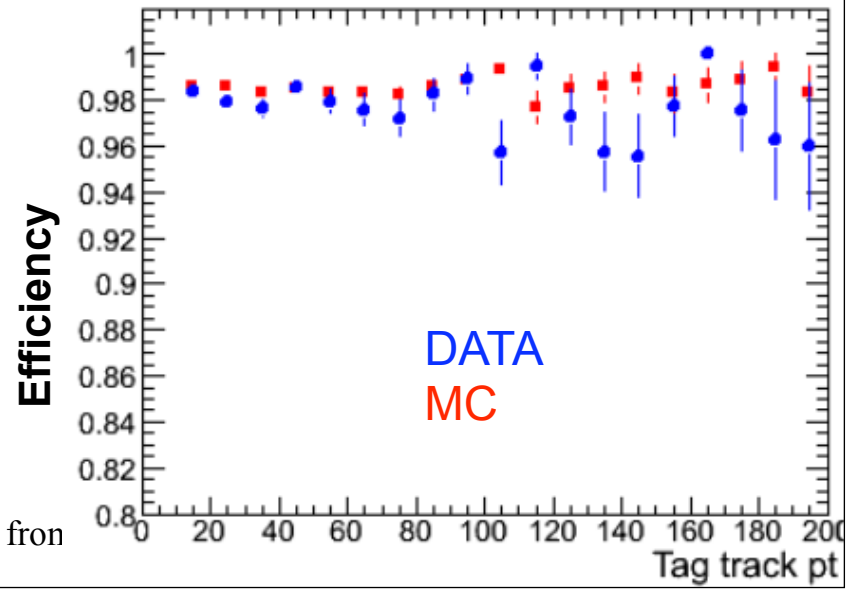

14. CMS Tracker : Lorentz angle

The magnetic filed in the CMS TK (3.8 T) changes the drift direction of the holes respect to the depletion field by θ_L.

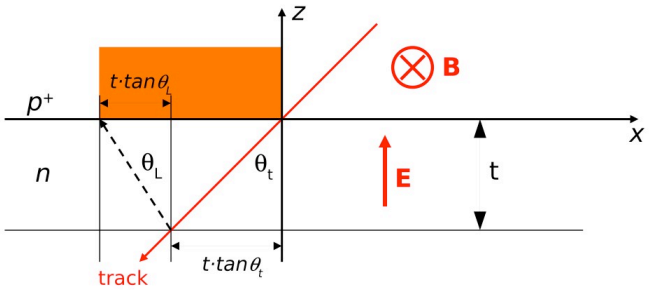

$$\Delta x = t \cdot \tan\theta_L$$

$$\tan\theta_L = \mu_H \cdot B$$

Plot cluster size vs incident angle of the track on the module.

Minimum of the distribution ⟶ θ_L

$<\mu_H>$ (TIB, 320 μm sensors) = 0.018 T^{-1}

$<\mu_H>$ (TOB, 500 μm sensors) = 0.023 T^{-1}

Different analyses techniques give compatible experimental results. Independent test from alignment confirms them.

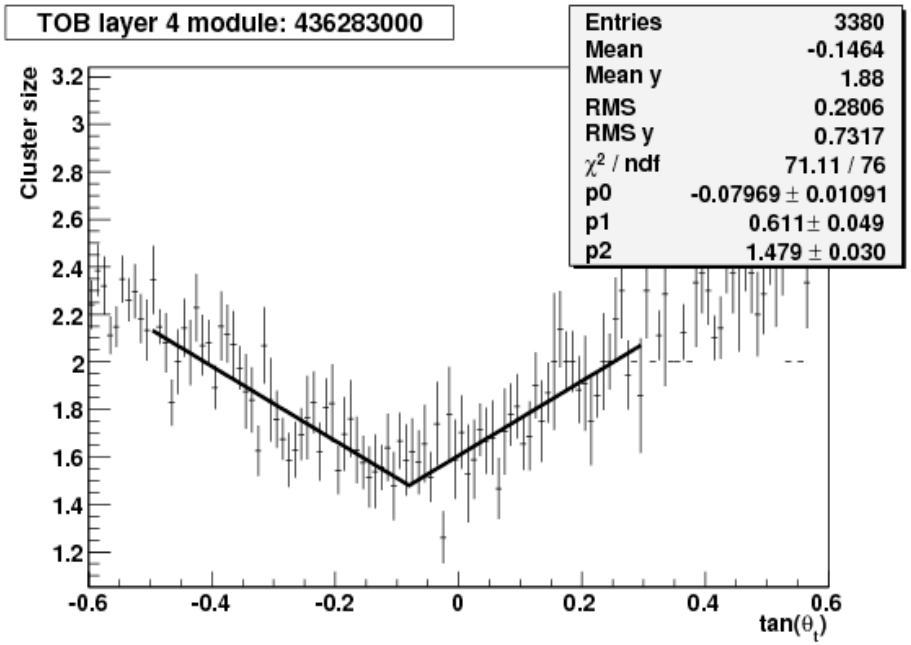

A. Bonato, Elba 2009

14. ATLAS Experiment

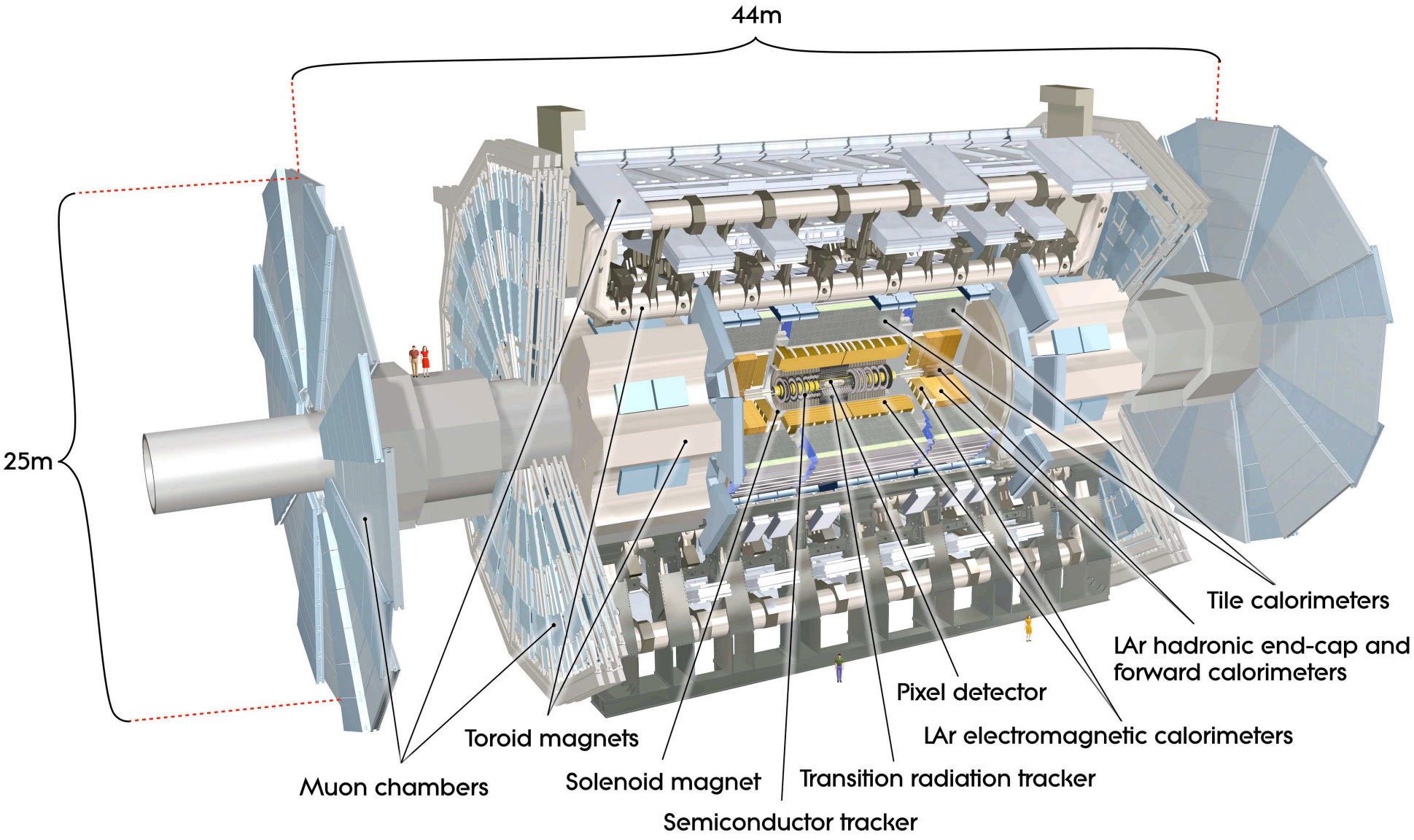

14. ATLAS Inner Detector

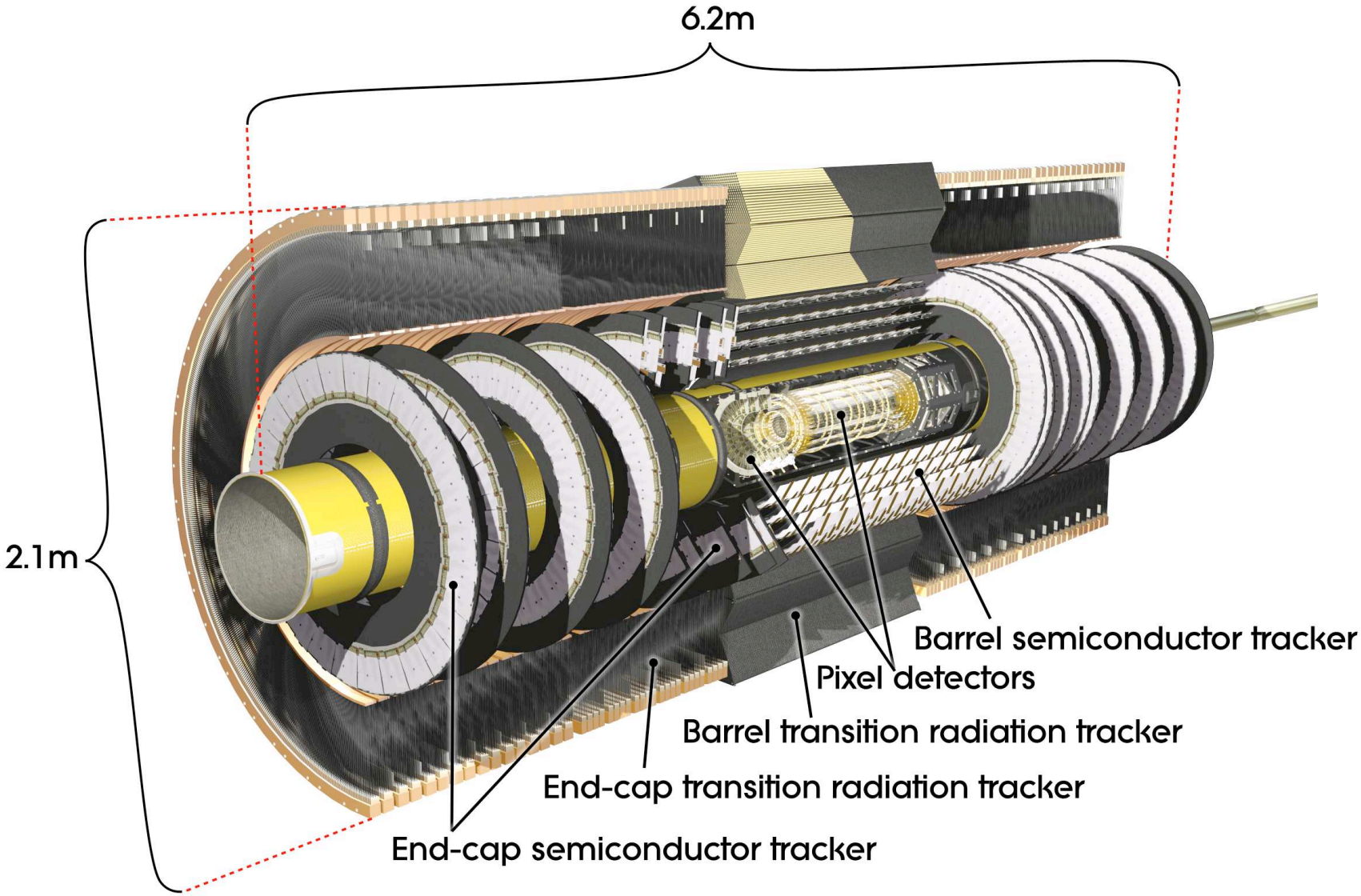

Cut-away view of the ATLAS inner detector.

14. ATLAS Inner Detector

Transition Radiation TRT

- 351 000 readout channels
- 36 hits per track
- 4 mm diameter straw tubes
- 144 cm long straws, divided in 2 halves
- accuracy 130 μm per straw
- endcap 37 cm long radial straws

Silicon Strip Tracker SCT

- 6.3 million readout channels

Barrel

- 8 strip layers (4 space points) per track
- stereo strips (40 mrad) parallel to z
- 6.4 cm long daisy chained sensors (80 μm pitch)
- accuracies 17 μm (R-ϕ), 580 μm (z)

Endcap

- set of radial strips
- set of stereo strips (40 mrad)
- mean pitch about 80 μm
- accuracies 17 μm (R-ϕ), 580 μm (

Pixel Detector

- 3 pixel layers
- Pixel size in R-ϕ × z: 50 × 400 μm^2
- Barrel accuracies are 10 μm (R-ϕ), 115 μm (z)
- Disk accuracies are 10 μm (R-ϕ), 115 μm (R)
- 80.4 million readout channels

14. ATLAS - Sensors traversed by charged track

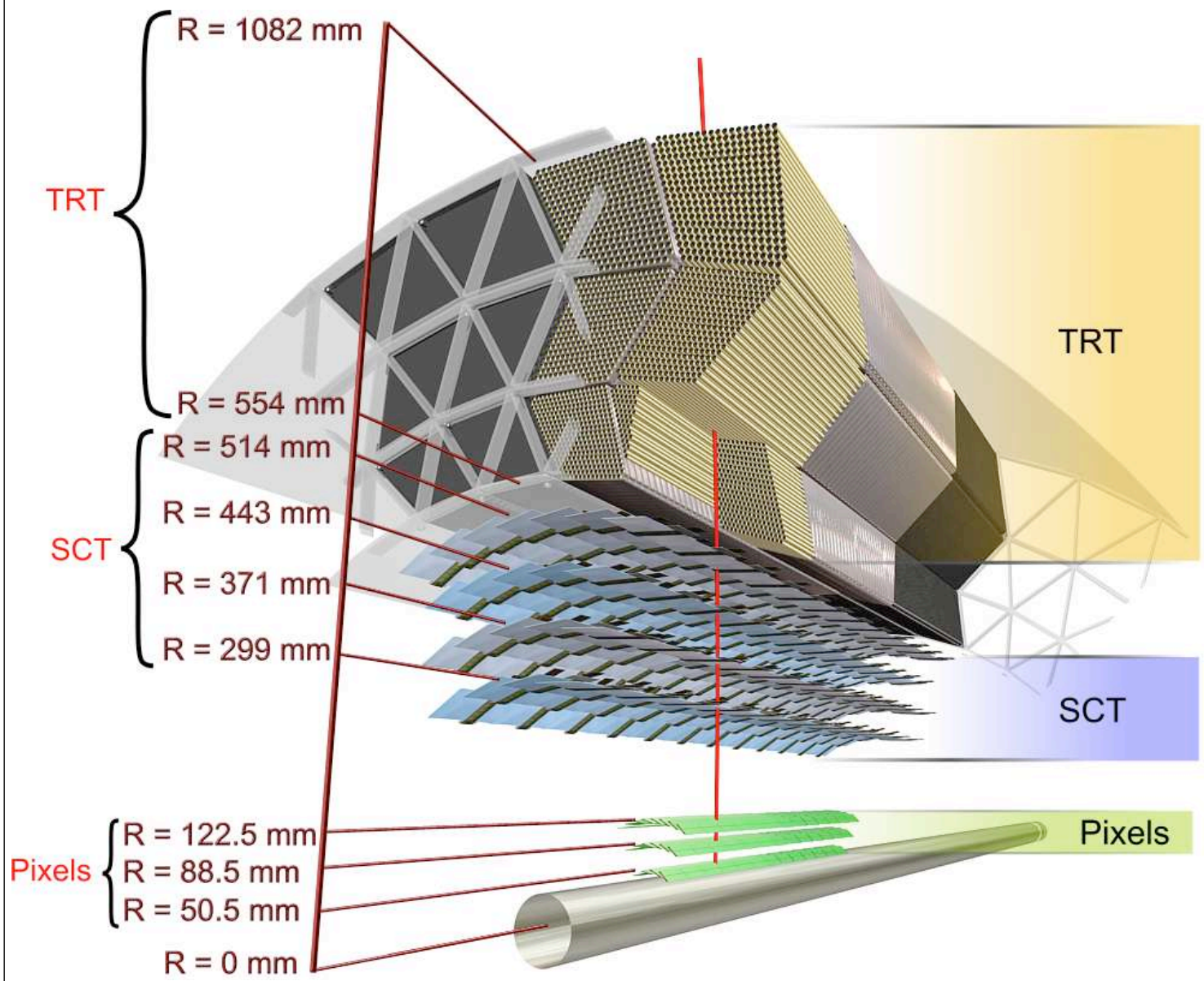

Charged track of $p_T = 10$ GeV at $\eta = 0.3$. traverses:

- beryllium beam pipe
- 3 pixel layers
- 4 double SCT layers
- about 36 TRT straws

14. ATLAS - Sensors in the Endcap

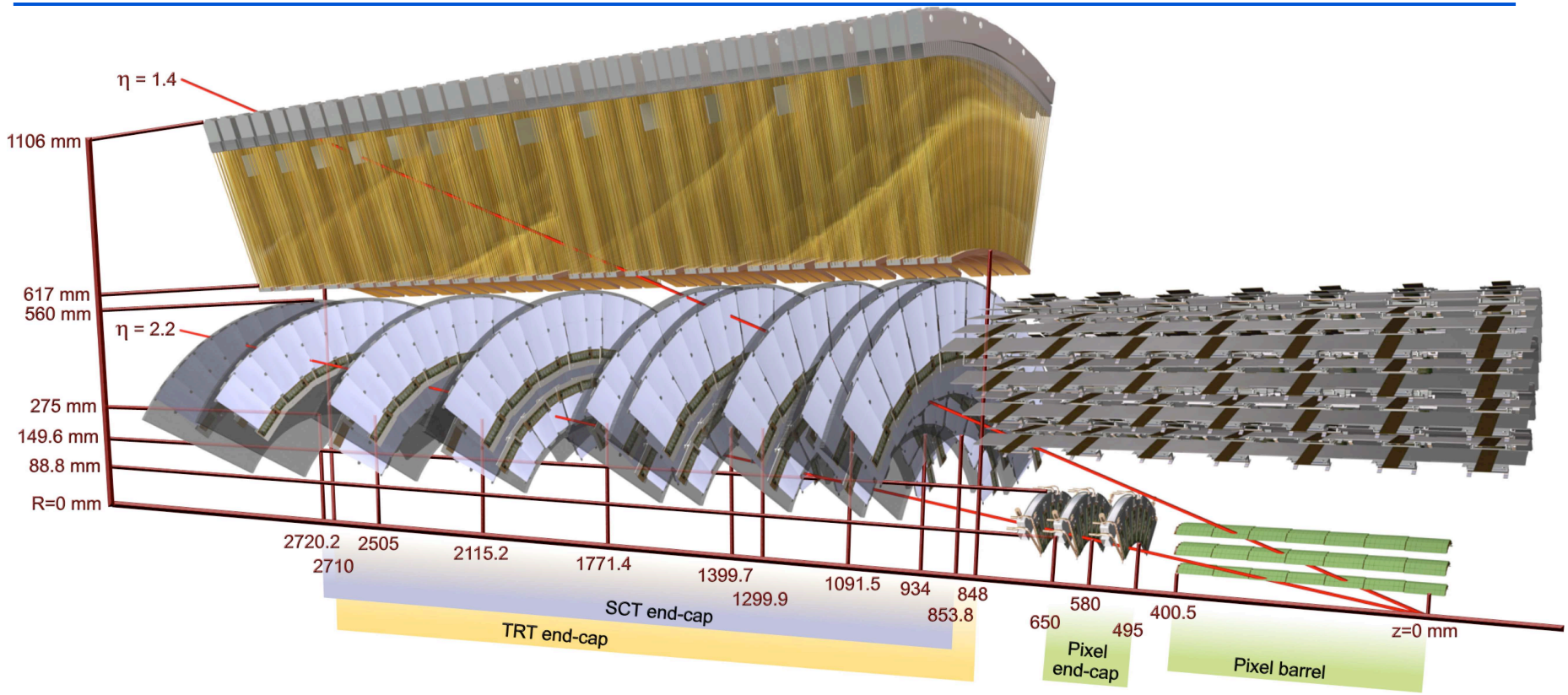

Charged track of p_T =10 GeV. It traverses

at η=1.4 : beryllium beam pipe, 3 pixel layers, 4 disks with double SCT layers, about 40 TRT straws.

at η=2.2: beryllium beam pipe, 1 pixel B-layer, 2 endcap pixel disks, 4 disks with double SCT layers, no TRT straws.

14. ATLAS - Barrel Pixel Module

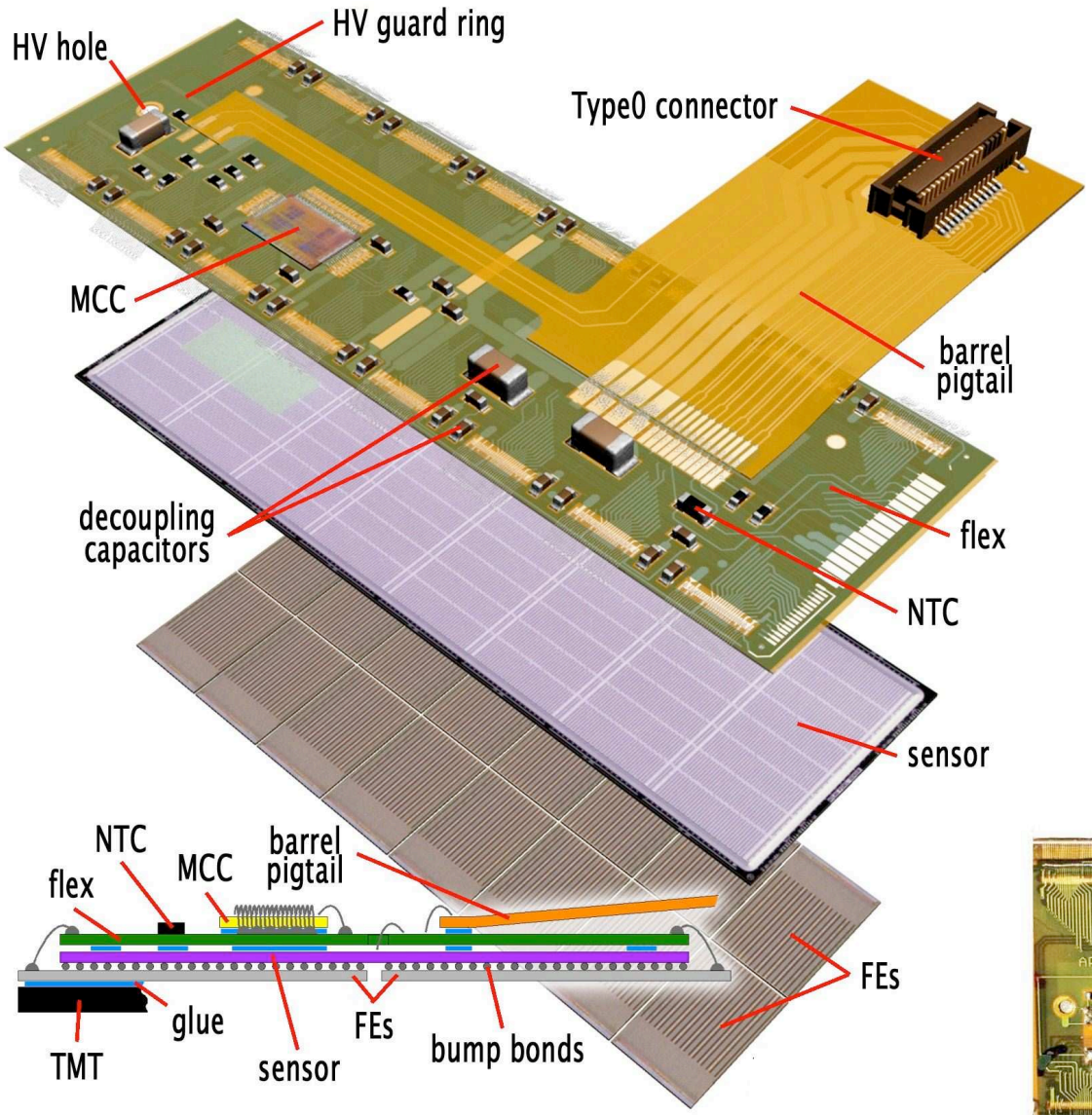

Pixel module:

Top: Hybrid, MCC control chip, NTC thermistor, HV element, Type0 connector

Midle: Sensors

Bottom: FE board

Bottom left: bump bonding between sensor and FE board.

Bottom right: photo of pixel module

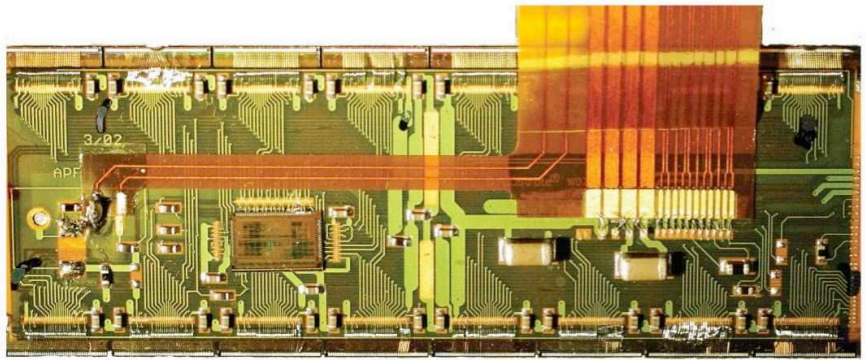

14. ATLAS - Transition Radiation Tracker (TRT)

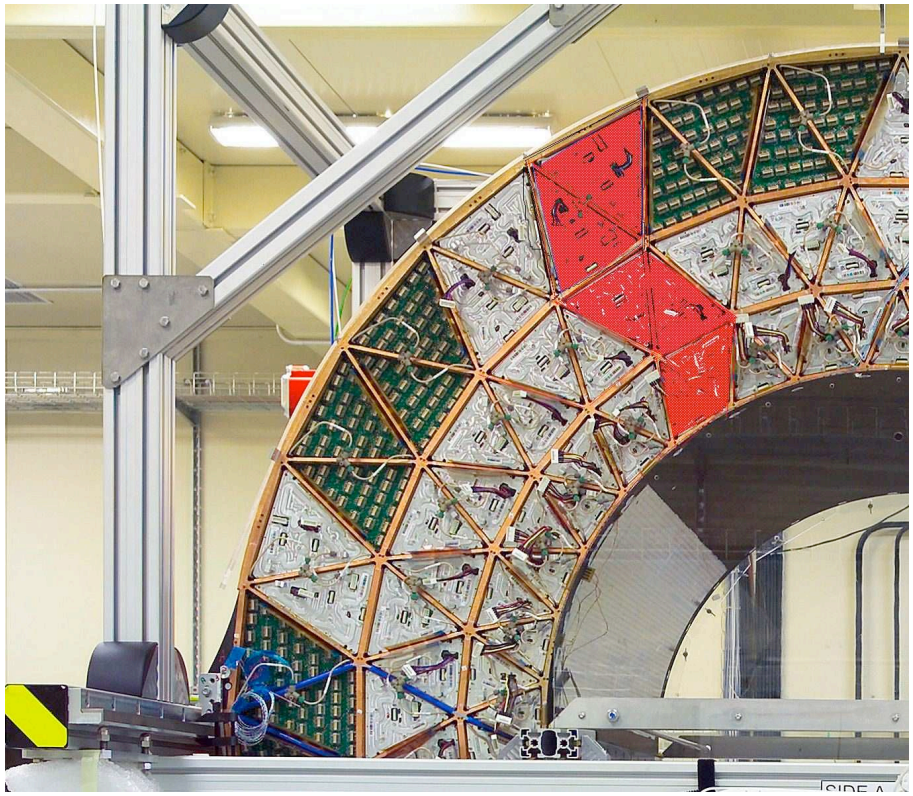

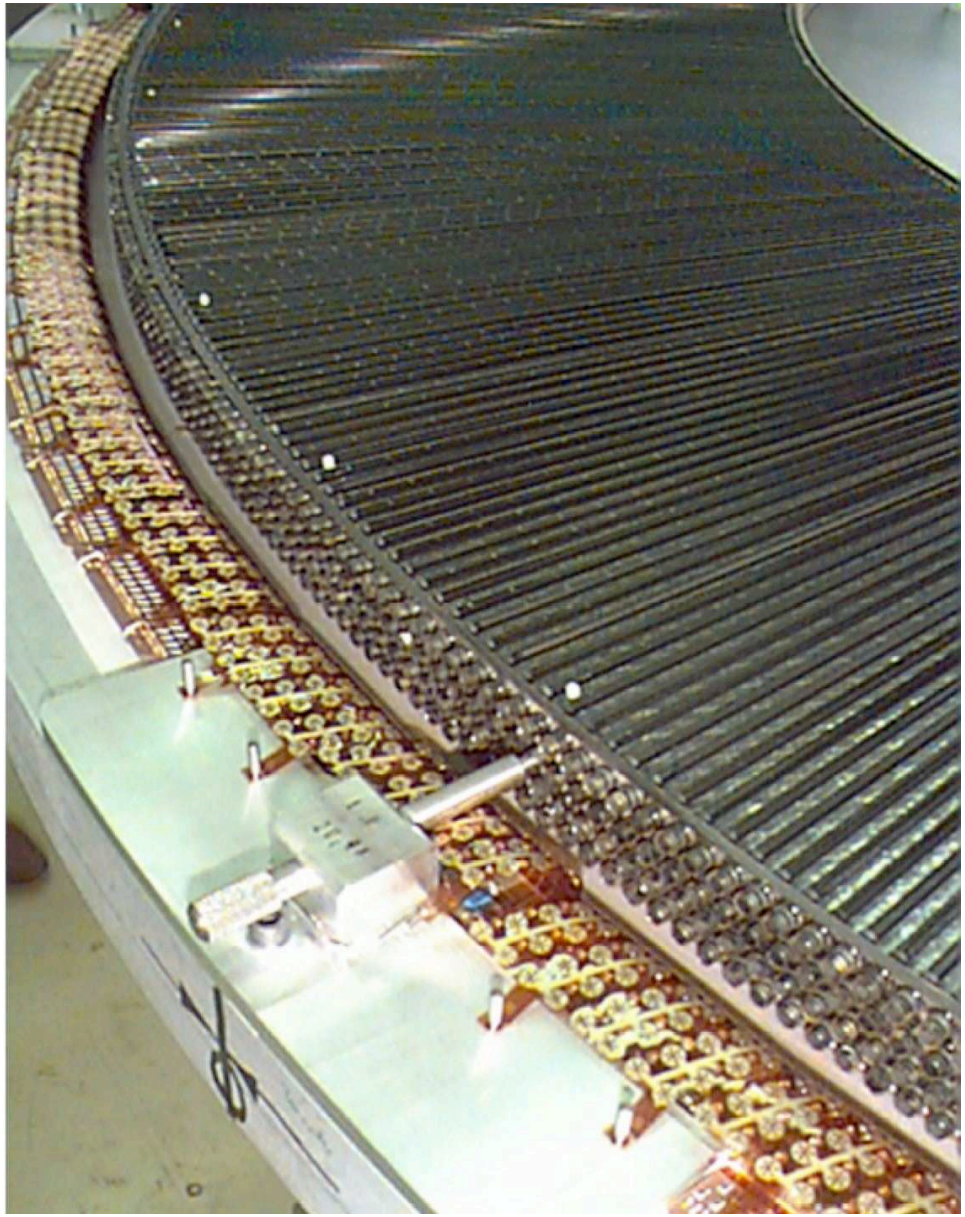

The transition radiator tracker consists of
gas filled straws and polypropylene radiator foils.

14. ATALS Pixel Support Structure

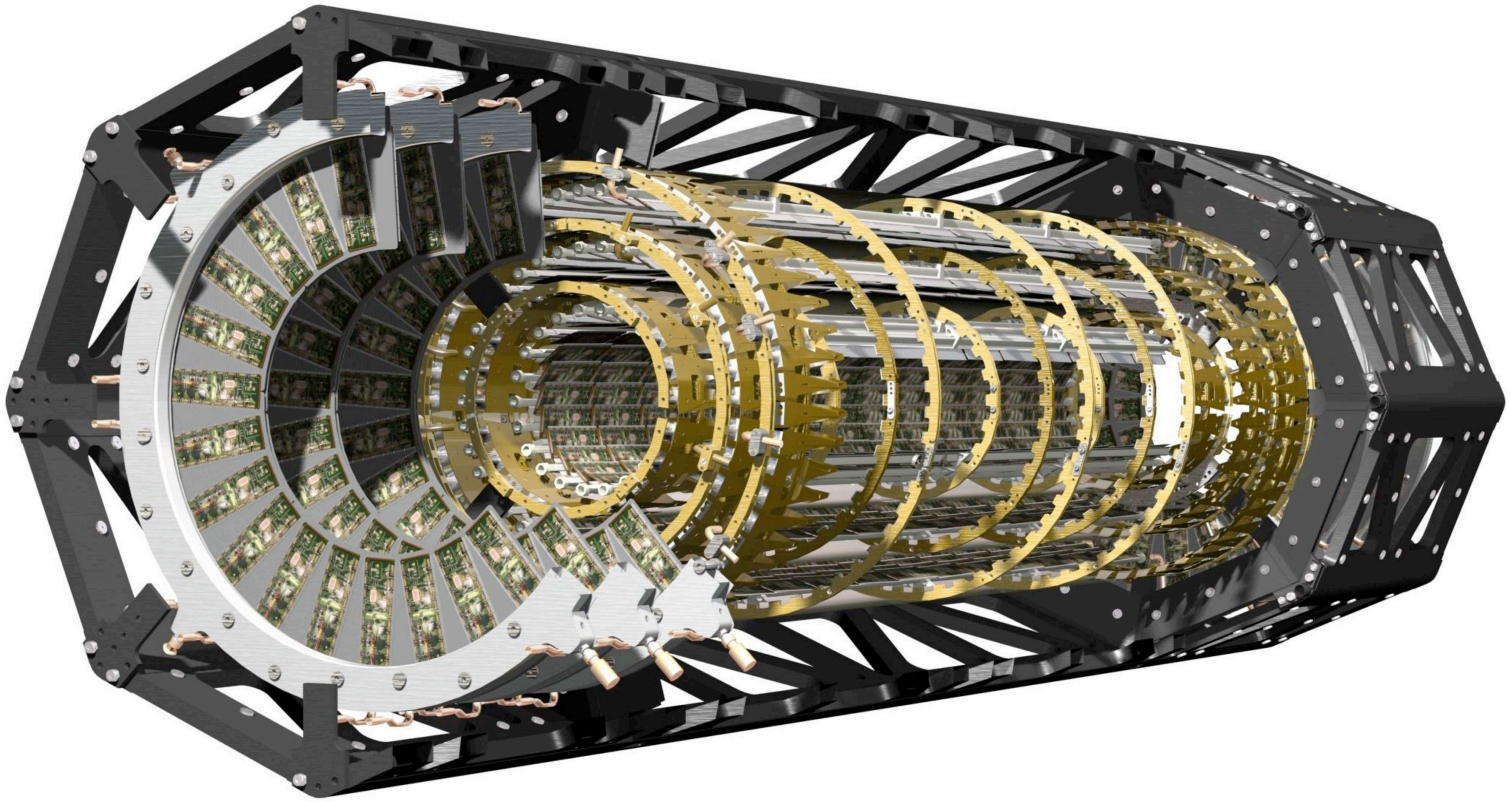

Figure 4.24: A perspective cut-away view of the pixel detector. The view shows individual barrel and end-cap modules, supported with their associated services on staves and disks within an octagonal support frame.

14. ATLAS Pixel Detector Integration

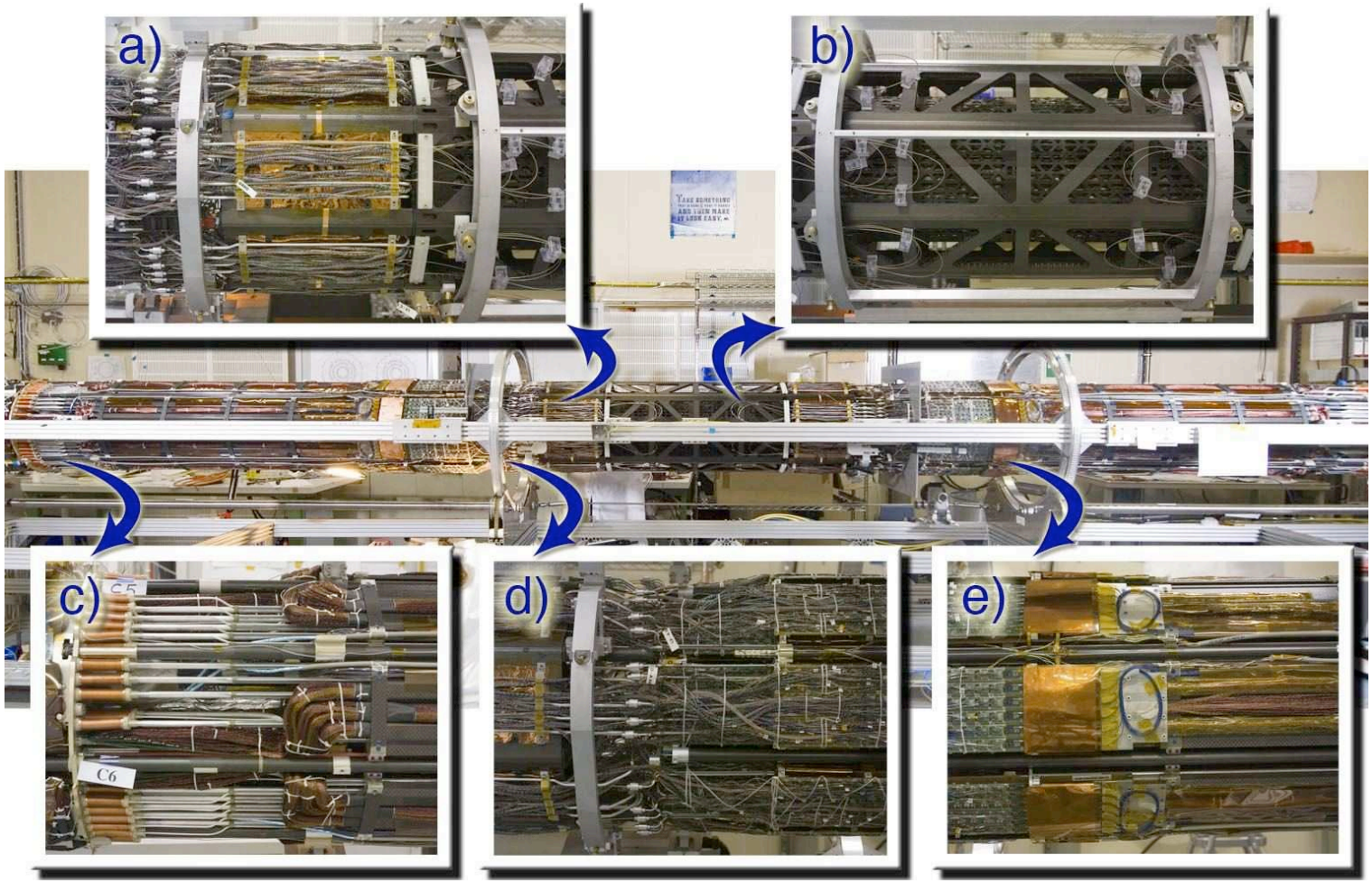

Figure 4.28: The pixel detector during integration of the barrel, end-caps and their services: (a) the end-cap region; (b) the barrel detector region; (c) Patch Panel 1 (PP1) region; (d) Patch Panel 0 (PP0) region and (e) region of the optical transceivers on the service quarter-panels. See text for details.

14. ATLAS Inner Detector Integration

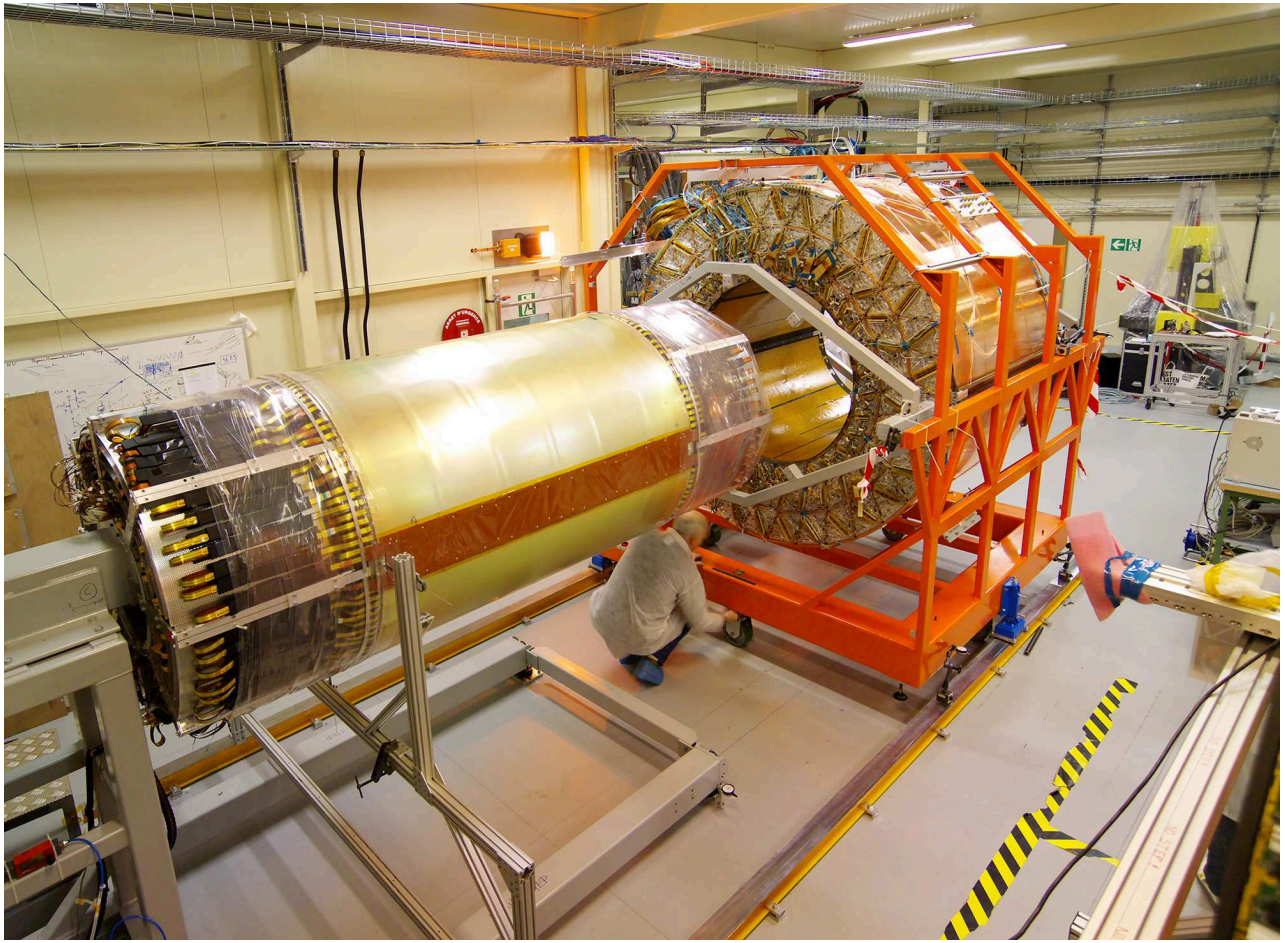

Figure 4.33: Insertion of SCT barrel into the TRT barrel. The three module types of the TRT barrel are clearly identified. The SCT outer thermal enclosure is visible, together with the barrel services extending on support frames from each end.

14. ATLAS Cosmic Event

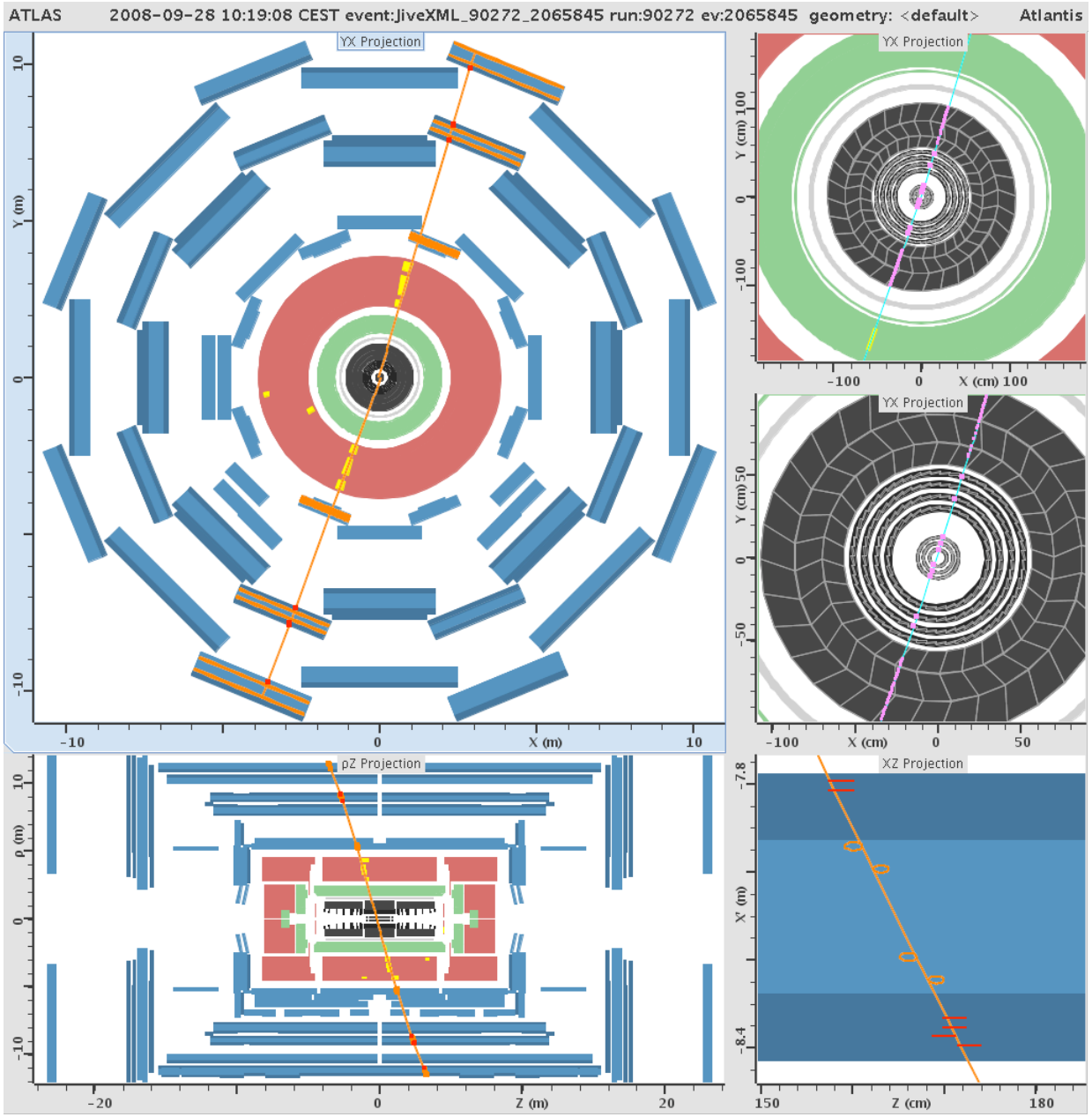

14. ATLAS ID : Event Displays

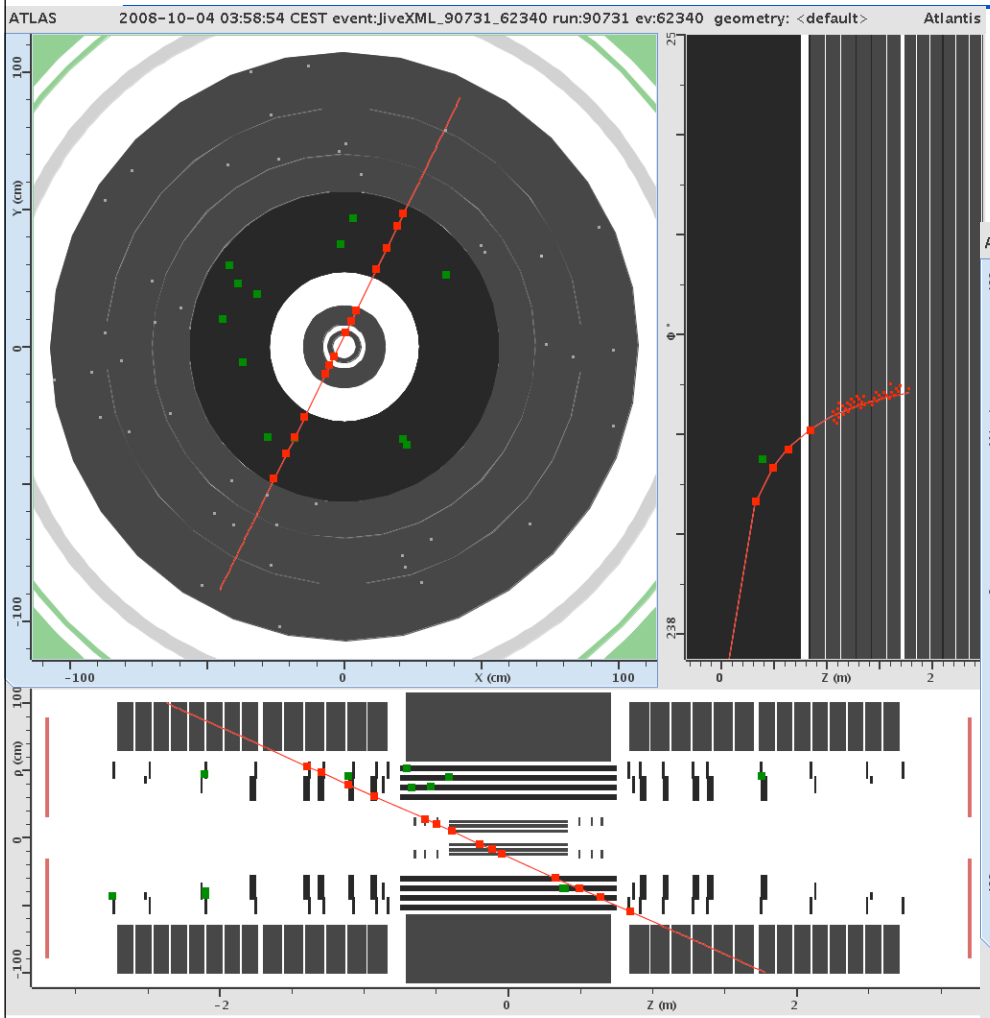

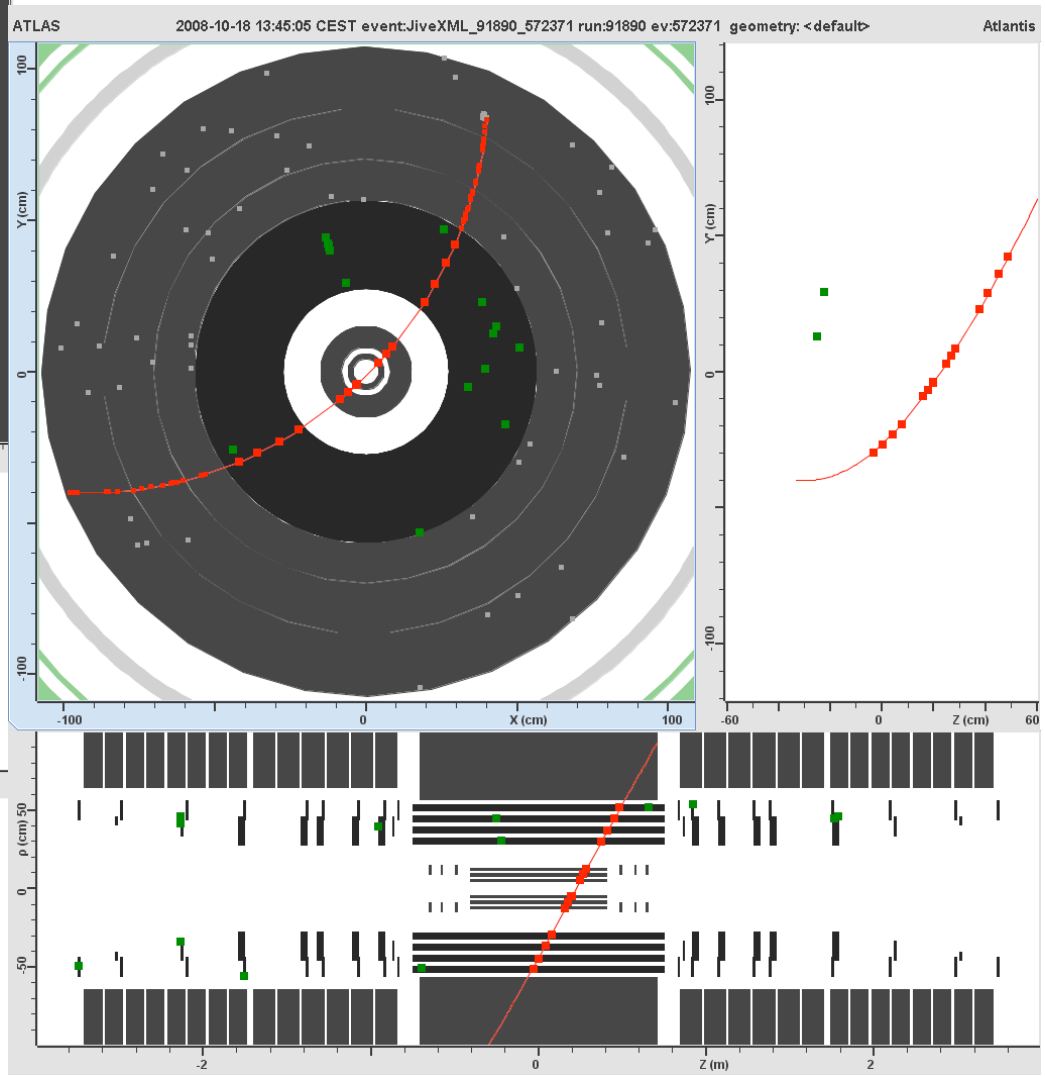

14. ATLAS SCT Performance

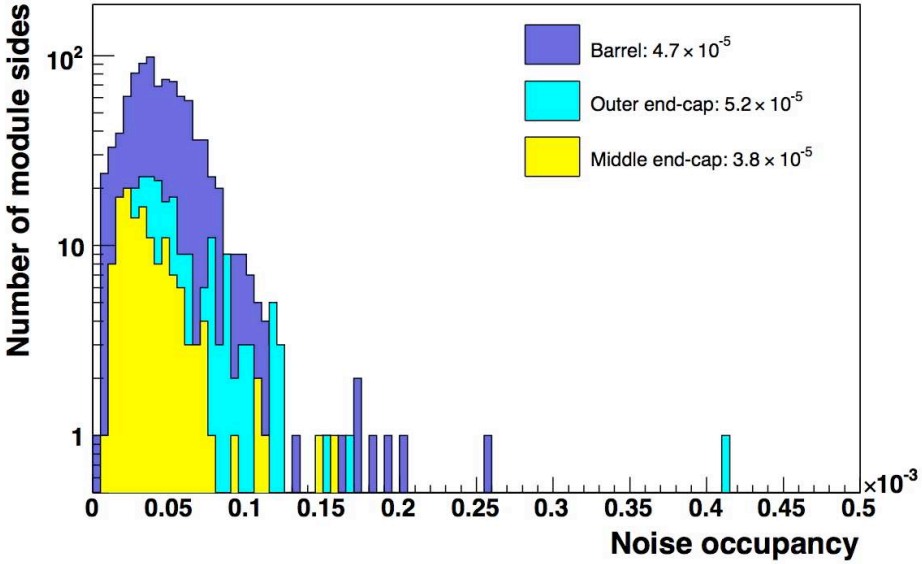

Figure 4.39: Distribution of average noise occupancy for all active module sides of the barrel and end-cap SCT (outer or middle end-cap modules on side C), as obtained at 1 fC threshold.

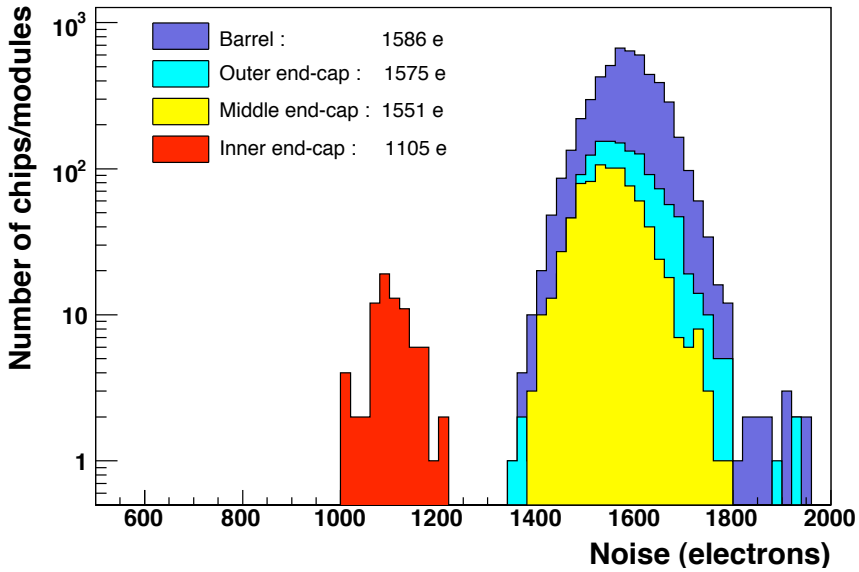

Figure 4.40: Distribution of the noise in electrons, normalised to a temperature of 0°C, for all active modules (or front-end chips) in the barrel and end-cap SCT (side C).

14. ATLAS Material budget

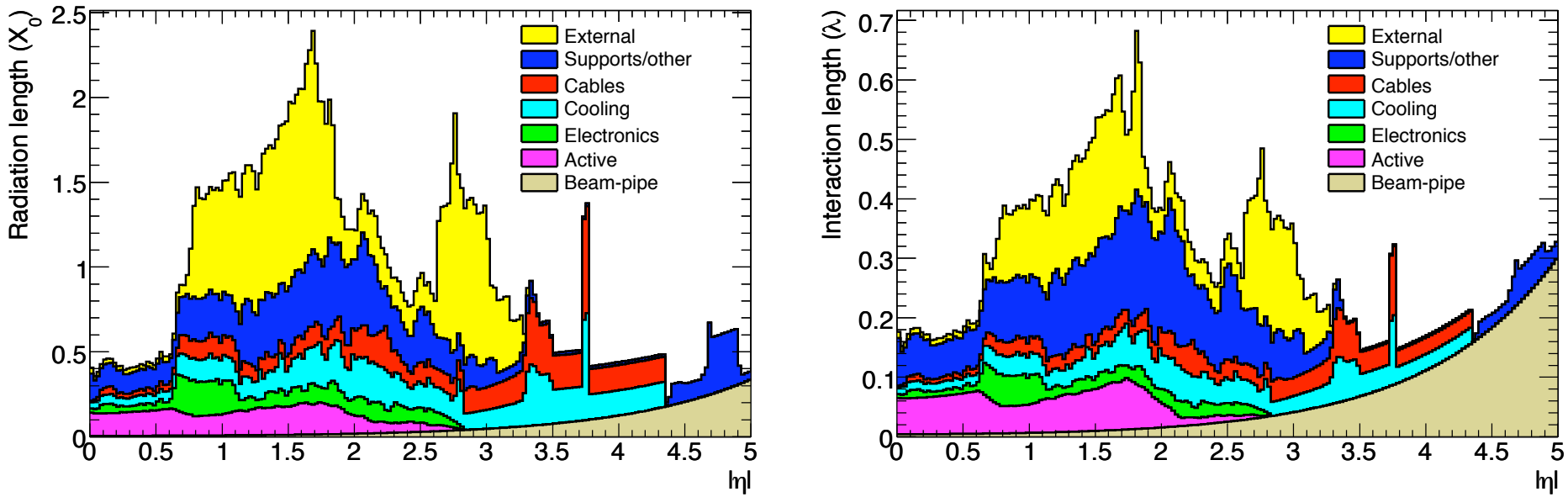

Figure 4.46: Material distribution (X_0, λ) at the exit of the ID envelope, including the services and thermal enclosures. The distribution is shown as a function of $|\eta|$ and averaged over ϕ. The breakdown shows the contributions of different ID components, independent of the sub-detector.

14. ATLAS Pixel Results: Cosmic Rays

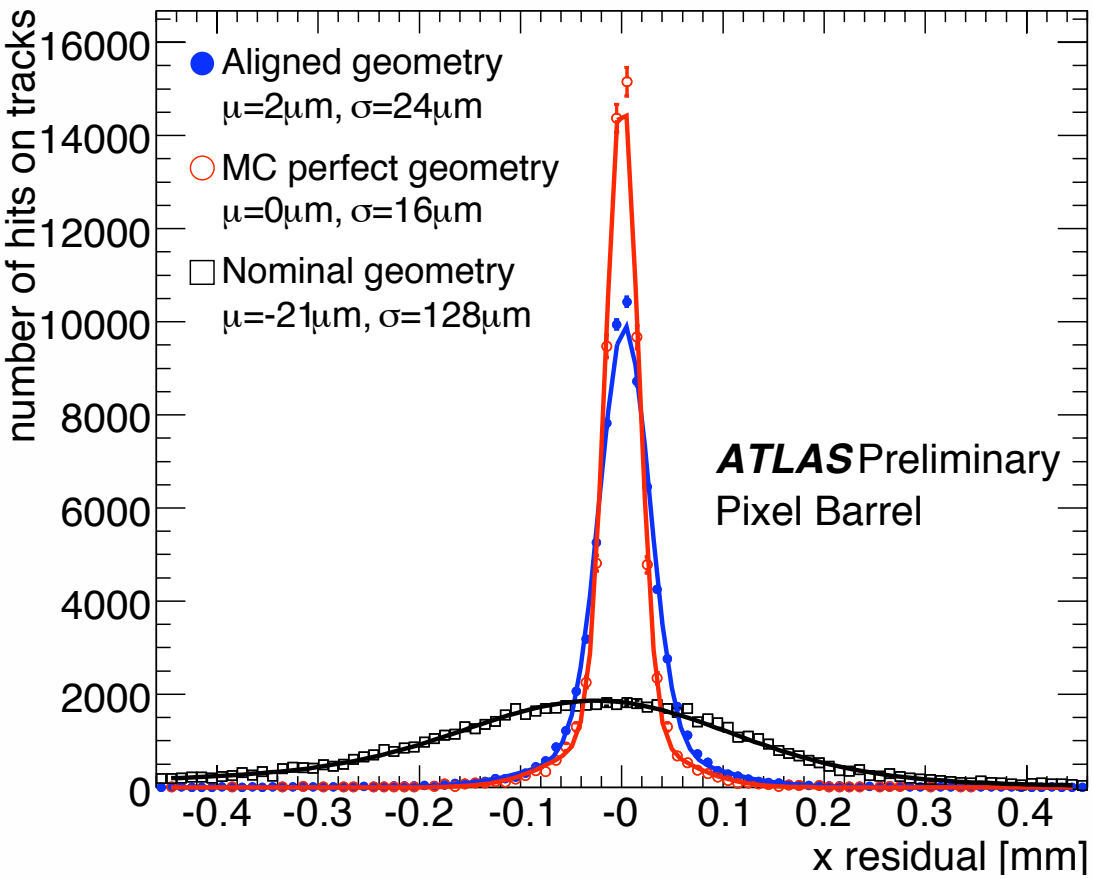

Residual distribution in x, integrated over all hits-on-tracks in the pixel barrel for the nominal geometry and the preliminary aligned geometry.

The residual is defined as the measured hit position minus the expected hit position from the track extrapolation. Shown is the projection onto the local x coordinate, which is the precision coordinate.

Tracks are selected to have pT > 2 GeV, |d0|<50mm, |z0|<400mm (in other words they are required to go through the pixel L0).

14. ATLAS ID Results: Cosmic Rays

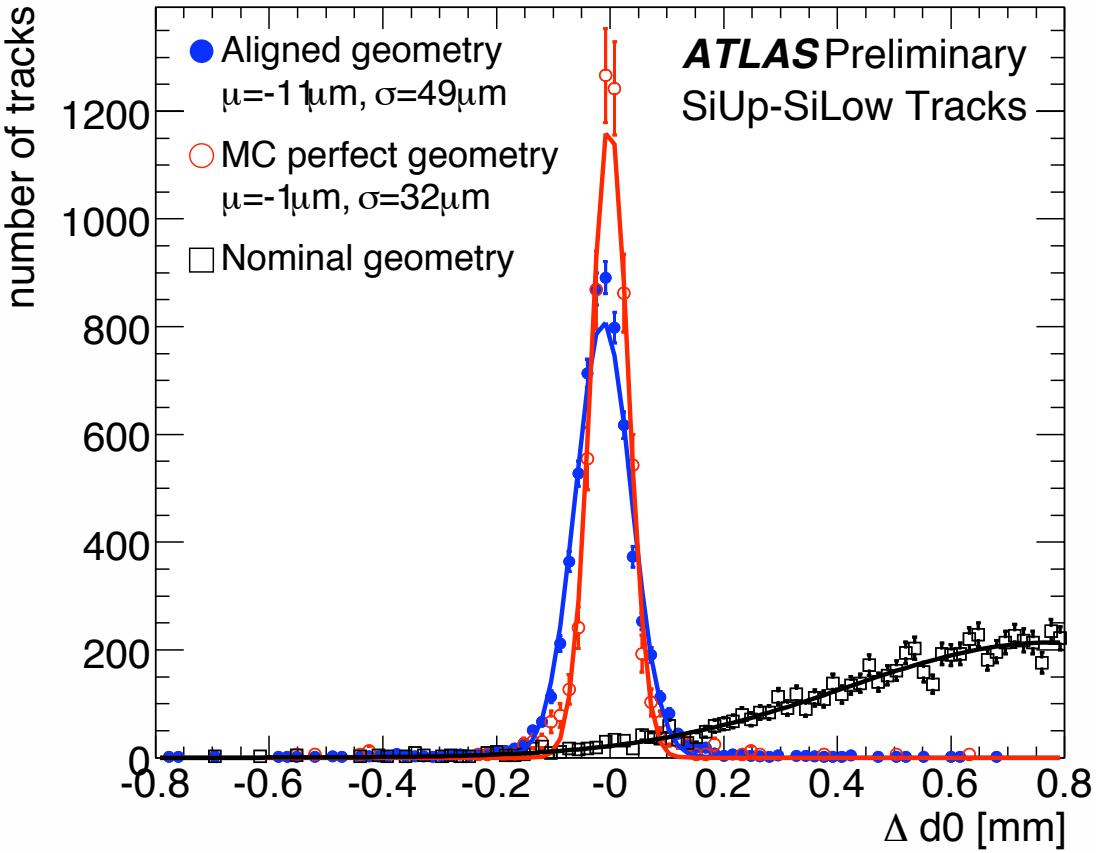

Cosmic tracks crossing the entire ID leave hits in both the upper and lower halves of the ID.

These tracks can be split near the interaction point and fit separately, resulting in two collision-like tracks that can then be compared.

The plots shows the difference in the d0 track parameter between the two split tracks. Tracks are selected to have pT > 2 GeV, |d0|<50mm, |z0|<400mm (in other words they are required to go through the pixel L0).

Tracks also are required to have a hit in the Pixel B layer, 3 Pixel hits and in total 7 Silicon hits.

Further Reading

General books about particle detectors:

W. R. Leo - Techniques for Nuclear and particle Physics Experiments

K. Kleinknecht - Detectors for Particle Radiation

C. Grupen - Particle Detectors

G. Lutz - Semiconductor Radiation Detectors

W. Blum, W. Riegler, G. Rolandi - Particle Detection with Drift Chambers

Online:
http://physics.web.cern.ch/Physics/ParticleDetector/BriefBook/